

SP1-JTI-CS-2013-02

Power cable modelling for WIPS
electromechanical chain

Project reference:
SGO-02-077 - MultyCaB - 632458

Deliverable 2

DEFINITION OF METHODOLOGY FOR POWER CABLE MODELLING

February 2015

PUBLIC

Subject: Deliverable 2

Document type: Public

Prepared by: UPC, Universitat Politècnica de Catalunya
MCIA Research Center



This page is left in blank intentionally



1	INTRODUCTION	6
1.1	CABLES TO BE MODELED AND TESTED	7
1.2	SUMMARY OF THE METHODOLOGY TO BE APPLIED TO MODEL AND TEST THE CABLES	8
2	THE HIGH-FREQUENCY MODEL OF DIFFERENT CABLES	11
2.1	LONGITUDINAL IMPEDANCE MODEL	11
2.2	TRANSVERSAL IMPEDANCE MODEL	12
2.3	CELL MODEL OF AN UNSHIELDED TWO-CONDUCTOR CABLE INCLUDING THE LONGITUDINAL AND TRANSVERSAL IMPEDANCES 12	
2.4	CELL MODEL OF A TWO-CONDUCTOR SCREENED CABLE INCLUDING THE LONGITUDINAL AND TRANSVERSAL IMPEDANCES..	13
2.5	CELL MODEL OF AN THREE-CONDUCTOR UNSCREENED CABLE INCLUDING THE LONGITUDINAL AND TRANSVERSAL IMPEDANCES	14
2.6	CELL MODEL OF A THREE-CONDUCTOR SCREENED CABLE INCLUDING THE LONGITUDINAL AND TRANSVERSAL IMPEDANCES	14
3	EXPERIMENTAL SETUP AND CABLE PARAMETERS DETERMINATION	16
3.1	THE IMPEDANCE ANALYZER TO CONDUCT THE EXPERIMENTAL TESTS	16
3.2	EXPERIMENTAL MEASUREMENT OF THE MODEL PARAMETERS OF A TWO-CONDUCTORS UNSCREENED CABLE.....	17
3.2.1	<i>Short circuit test in a two-conductors unscreened cable.....</i>	17
3.2.2	<i>Open circuit test in a two-conductors unscreened cable.....</i>	18
3.3	EXPERIMENTAL MEASUREMENT OF THE MODEL PARAMETERS OF A THREE-CONDUCTORS UNSCREENED CABLE.....	18
3.3.1	<i>Short circuit test in a three-conductor unscreened cable</i>	19
3.3.2	<i>Open circuit between test in a three-conductors unscreened cable.....</i>	20
3.4	EXPERIMENTAL MEASUREMENT OF THE MODEL PARAMETERS OF A TWO-CONDUCTORS SCREENED CABLE.....	20
3.4.1	<i>Short circuit tests in a two-conductors screened cable (CM and DM).....</i>	21
3.4.2	<i>Open circuit between test in a two-conductors screened cable (CM and DM)</i>	22
3.5	EXPERIMENTAL MEASUREMENT OF THE MODEL PARAMETERS OF A 3-CONDUCTORS SCREENED CABLE	23
3.5.1	<i>Short circuit tests.....</i>	23
3.5.2	<i>Open circuit tests.....</i>	24
3.6	MODEL PARAMETERS IN THE RANGE 40 Hz- 40 MHz.....	25
4	GA-BASED ITERATIVE ALGORITHM TO ADJUST THE COEFFICIENTS OF THE IMPEDANCE NETWORK FROM THE MEASURED FREQUENCY RESPONSE OF THE CABLE	29
4.1	MODELLING THE LONGITUDINAL IMPEDANCE OF AN ISOLATED CONDUCTOR.....	32



4.2	MODELLING THE TRANSVERSAL IMPEDANCE OF AN ISOLATED CONDUCTOR	34
5	R, L AND C ELEMENT MODELS	37
5.1	TRAPEZOIDAL RULE OF INTEGRATION	37
5.2	RESISTANCE MODEL	37
1.1	INDUCTANCE MODEL	38
5.3	CAPACITANCE MODEL	39
5.4	INTEGRATION RESULTS SUMMARY	40
6	NODAL ANALYSIS COMBINING R, L AND C ELEMENTS	42
6.1	CONDUCTANCE MATRIX INVERSION	42
6.2	NODAL CIRCUIT ANALYSIS. EXAMPLE.....	42
6.3	LONGITUDINAL AND TRANSVERSAL IMPEDANCES OF A TWO-CONDUCTORS UNSCREENED CABLE. SINGLE CELL MODEL	43
7	CONCLUSIONS	47
8	REFERENCES	48



Introduction



Document	Deliverable 2
Facilities	-
Revision	Revised
Date	February 2015

1 Introduction

Several promising technologies are being explored and developed by Clean Sky, ranging from power generation, distribution, and conversion systems, resulting in an architecture that became more and more complex and have to be optimized to substantially reduce the consumption of non-propulsive power. One of such technologies likely to be optimized is the electrical **Wing Ice Protection System (WIPS)**, which protect against the build-up of ice on structures of the aircraft. During flight, the surfaces of an aircraft can be exposed to water vapor at low temperatures and, if no preventative action is taken, ice can quickly form on the wings, on control surfaces, and on other parts of the aircraft in such a way as to alter the aerodynamic performances with potentially catastrophic consequences.

Among the thermal ice protection systems, electro-thermal anti-icing are simple and compact methods and their response time is very short compared to hot air or chemical systems, allowing for intermittent or cyclic heating. Electrical resistance heating systems in aircraft industry are mostly used in the form of electro-thermal pads. These electro-thermal pads are applied onto the surface of a structure or as close as possible to the skin surface to heat the surface and prevent ice accretion. Currently, they are one of the main ice protection technologies that are being integrated and tested.

The electro thermal WIPS works by embedding the electro-thermal heater mats into the surface to be protected, for instance, the interior surface of the composite slat leading edge skin. An electronic controller monitors the condition of each surface individually, and controls the power electronics that supplies the power to the heater element, which could be AC or DC, depending upon the particular customer installation requirement.

However, the natural switched operation of solid state technology introduces new challenges related to switching frequencies, switched voltage and (sometimes) switched current on the electric and electronic circuits of the aircraft, including of course the wiring for the Electrical Wiring Interconnection System (EWIS) of the aircraft and specifically for the WIPS.

With the power converter operating as ON-OFF, unipolar and bipolar PWM, switched AC or DC voltage source, etc., new effects such as switching and commutation harmonics, skin effect, high dv/dt , EMI, etc., need to be considered and conveniently modelled on basic the cable model. This advanced cable model will facilitate the analysis of the complete EWIS system simulations with high degree of accuracy, and will contribute to the development of new WIPS minimizing design errors and helping to components specification.

The analysis and evaluation of these effects will lead to define and develop a Multi Layer Cable Model, **MultyCaB**, able to analyze steady state and transients, fundamental and harmonic behavior, thermal effects, high frequency modelling and skin effect, and dv/dt effects.

Due to the features of the PWM-modulated switching voltage applied to the cable, the cable model has to include low and high frequency effects, and must be able to simulate reflected waves due to high dv/dt transients.

The new power cables at the aircraft connect the loads with power suppliers or electrical high voltage buses mainly through electronic power converters. It means that power cables support commutated, high voltage AC or DC voltage whereas transport high ripple currents to the aircraft loads, among which are the mats for WIPS. Therefore, basic cable models are not appropriate for simulations.

This is because modern IGBT-based converters have modulation frequencies in the range of 2 to 20 kHz with typical switching times of 50 ns or about 13 V/ns for a 460 V system. These operating conditions induce high voltage variations (dv/dt) which in turn excite the parasitic elements of the cables and mats, so to simulate the system behavior a high frequency model is required.

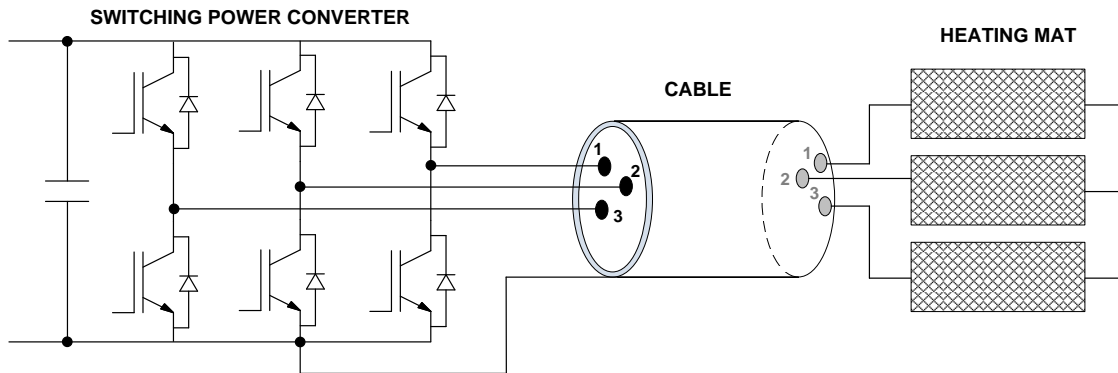


Fig. 1.1. Converter, cable and heating mat.

At high frequency, when dealing with power cables the eddy effects arise, so they have to be included in the cable model. Similarly, capacitive interactions between different cables and between cables and screen also happen. Therefore, to include these effects in the cable model, both a longitudinal impedance and a transversal impedance are included in the cable model. The parameters of these impedances have to be measured by means of a precision high-frequency impedance analyzer by applying two test types, that is, short circuit and open circuit tests to a short sample of the cable to be characterized in order to ensure that the model is able to reproduce the real cable response for a wide range of frequencies of 40 Hz – 40 MHz.

1.1 Cables to be modeled and tested

Since there are different cable configurations, two types of cables will be modeled and tested, although the procedure to model and test the cables detailed in the next sections of this report can be applied to other cable configurations.

- **Cable 1. Two-conductors unscreened cable**

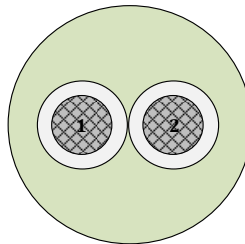


Fig. 1.2. Two-conductors unscreened cable.

- **Cable 2. Three-conductors screened cable**

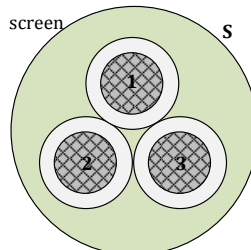
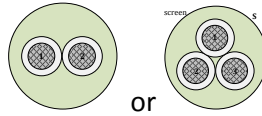


Fig. 1.3. Three-conductors screened cable.

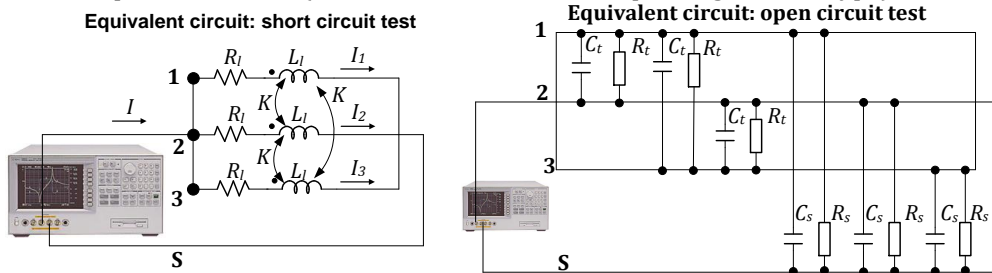
1.2 Summary of the methodology to be applied to model and test the cables

The next lines summarize the steps required to model and test any cable configuration.

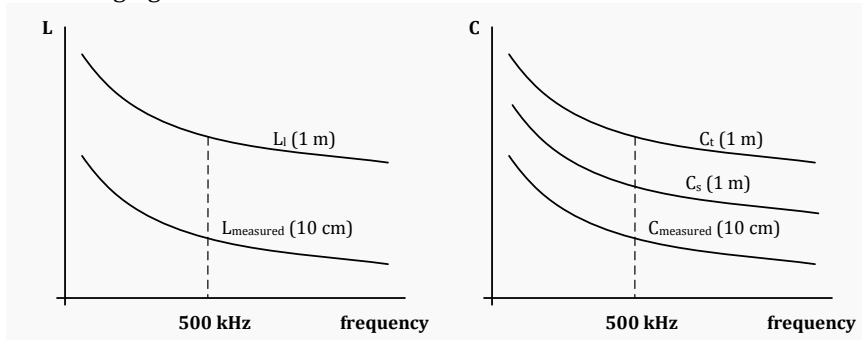
Step 1. Choose cable configuration.



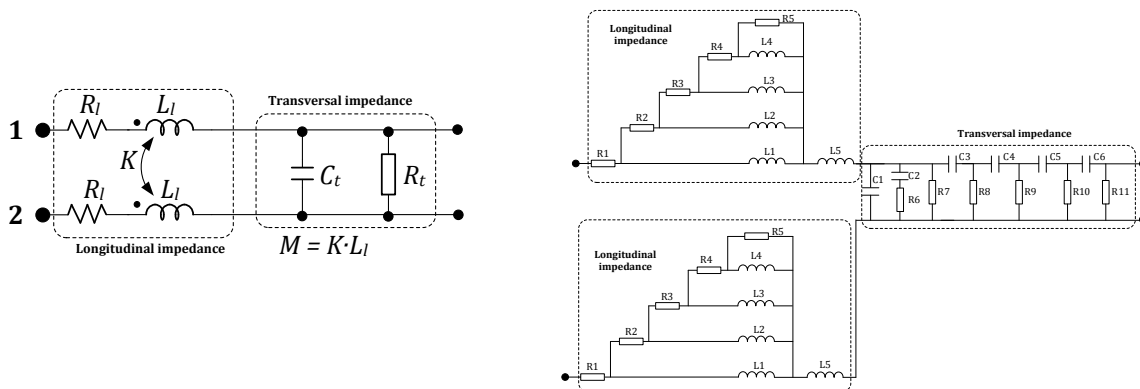
Step 2. Determine longitudinal and transversal parameters at 500 kHz (L_b , R_b , C_b , G_t , C_s and G_s is) from short circuit and open circuit tests (several tests, the number depending on cable type).



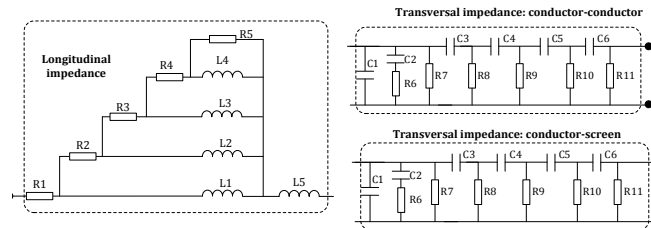
Step 3. Perform experimental short circuit and open circuit tests at 40 Hz – 40 MHz to determine $L_{measured}$, $R_{measured}$, $C_{measured}$ and $G_{measured}$. Only two tests are required. From these tests the frequency response of longitudinal and transversal cable parameters L_b , R_b , C_b , G_t , C_s and G_s is extrapolated as indicated in the following figures.



Step 5. Create 1-cell cable model including longitudinal and transversal impedances with **variable number of branches** in both longitudinal and transversal impedances. Next, use **Genetic Algorithm (GA) optimization** to determine the components of the longitudinal and transversal parameters (R_i , L_i , C_i and G_i with $i = 1...5$ or 6) to match the frequency response of the cell model with the experimental one of L_b , R_b , C_b , G_t , C_s and G_s .

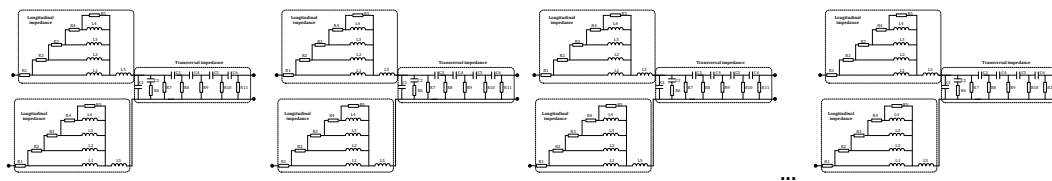


Document	Deliverable 2
Facilities	-
Revision	Revised
Date	February 2015



Note that when analyzing, for instance the longitudinal impedance, if the GA doesn't converge for a given number of branches, more branches have to be added to the analyzed impedance model until convergence is achieved.

Step 6. Generate a multi-cell circuit depending on cable length.



Step 7. Solve the circuit by applying nodal analysis combined with the differential equations solver. The input voltage must be that provided by the power converter.

This 7 steps procedure summarized above is explained in detail in the following sections.



MULTYCAB

February 2015 Deliverables 2

Document	Deliverable 2
Facilities	-
Revision	Revised
Date	February 2015

The cable model



Document	Deliverable 2
Facilities	-
Revision	Revised
Date	February 2015

2 The high-frequency model of different cables

Due to the features of the PWM-modulated switching voltage applied to the cable, the cable model has to include low and high frequency effects, and must be able to simulate reflected waves due to high dv/dt transients. Modern IGBT-based converters have modulation frequencies in the range of 2 to 20 kHz with typical switching times of 50 ns or about 13 V/ns for a 460 V system. These operating conditions induce high voltage variations (dv/dt) which in turn excite the parasitic elements of the cables and mats.

It is known that the mathematical function to describe the frequency dependence of the equivalent impedance $Z(f)$ in a cable is very complex and often unpractical to be applied when analyzing a wide-frequency interval, so an approximated high-frequency equivalent circuit is required [Sen1998,DePaula2008].

To fulfill the requirements of such a problem, it is necessary to implement a high-frequency multi-cell model, in which all the cells have identical parameters. It allows taking into account transients phenomena, skin and proximity effects and dielectric losses [Watson2003, Gudmundsdóttir2010]. The specific circuit in each cell, as well as the number of cells, must be adapted to each specific cable configuration. It is known that the distributed parameter representation of the transmission line can be used to analyze the overvoltage phenomena if an adequate number of cells is used in the calculation.

Power losses in a cable are due to different causes:

- **Copper losses.** They are due to the resistance of the conductor ($I^2 \cdot R$).
- **Dielectric losses.** They are caused by the voltage across the insulation.
- **Sheath losses.** They are due to the induced currents in the sheath.
- **Inter-sheath losses.** Caused by circulating currents in loops formed between sheaths of different phases.

Dielectric losses are voltage dependent, while the other losses are current dependent. Power losses affect not only the efficiency of the energy transport, but also the heating of the cable, which in turns affects the thermal behavior and resistance.

For this purpose the conductor may be regarded as composed of concentric shells. In the limit, at very low frequency, all the shells are carrying currents thus the conductor resistance is minimum and its internal inductance is maximum. However, when the frequency increases, the most inner shells gradually turn off, so only the outer shells remain active, therefore decreasing the internal inductance (reactance) while increasing the resistance.

The equivalent circuit to simulate each cell consists of two basic circuits:

- **Longitudinal impedance.** It includes two elements connected in series: a resistance and an inductance. However, to include the effects of high frequency components, different layers are assumed to deal with the skin effects. The resistance of the external connections as well as that of the conductor is represented by R_l . The inductance L_l accounts for the inductance presented in the conductors.
- **Transversal impedance.** It includes two elements connected in parallel: a resistance and an inductance. The shunt capacitive component C_t represents the dielectric property of the conductor insulation, and the resistive R_t component represents the dielectric loss.

2.1 Longitudinal impedance model

Each cell in the conductor may be regarded as composed of concentric shells. In the limit, at very low frequency, all the shells are carrying currents, thus the conductor resistance is minimum and its internal inductance is maximum. However, when the frequency increases, the most inner shells gradually turn off, so only the outer shells remain active, therefore decreasing the internal inductance (reactance) while increasing the resistance. The equivalent circuit shown in Fig. 2.1 models this effect and it is the approach to be used in each cell for the high-frequency model.

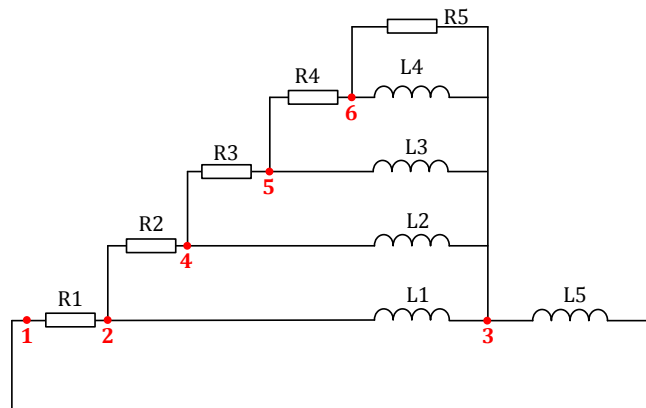


Fig. 2.1. Longitudinal impedance model.

By increasing the number of RL branches in the circuit shown in Fig. 2.1, the model bandwidth is increased.

2.2 Transversal impedance model

It is known that the response of dielectric materials to an electric field depends on its frequency, since the polarization effect experimented by the material is not instantaneous. When a dielectric withstands a time-varying electric field, a portion of the energy stored in the electric field is dissipated within the dielectric. This is because during the polarity change, the charges within the dielectric are displaced through the dielectric first in one direction and then in the other. Therefore, these charges encounter a certain opposition that leads to the production of heat, i.e. producing **dielectric loss**. Dielectric loss may be modeled by using the Debye model or a similar one, which is quite suitable in time-domain simulations, since it allows simulating the frequency-dependent material behavior by using an RC type equivalent-circuit model. Therefore, multi-branch shunt models composed of R and C elements, such as the Debye model, are often applied to model a lossy capacitor [Grzybowski2008,Engin2010].

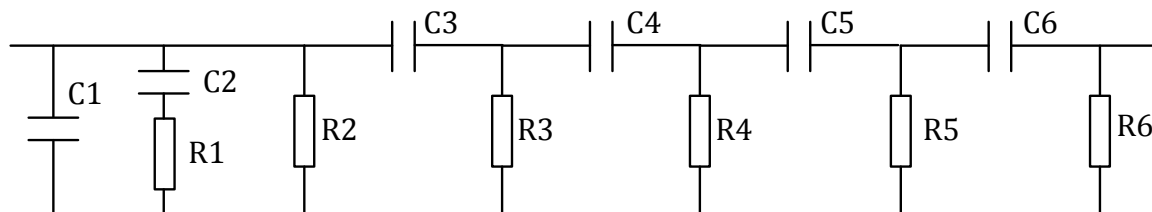


Fig. 2.2. Transversal impedance model.

By increasing the number of RC branches in the circuit shown in Fig. 2.2, the model bandwidth is increased.

2.3 Cell model of an unshielded two-conductor cable including the longitudinal and transversal impedances

Fig. 2.3 shows the electric equivalent circuit for wide-range frequency operation of a cell. Note that the full conductor consists of n cells/meter.

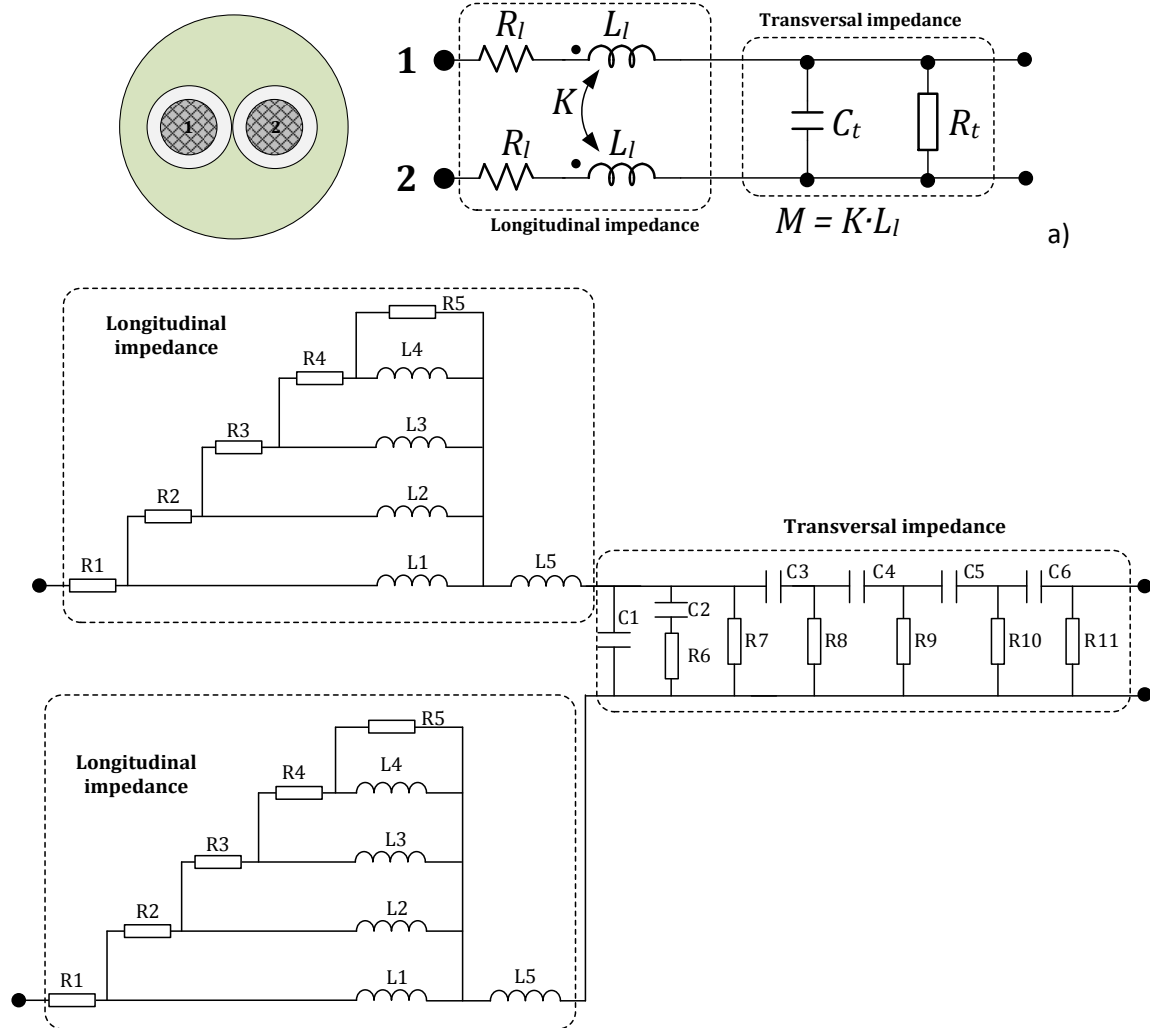


Fig. 2.3. Cell model for a two-conductor unscreened cable. a) Equivalent circuit. b) Detailed wide-frequency equivalent circuit.

Therefore, the circuit shown in Fig. 2.3 corresponds to the full model of a single cell for a two-conductor unscreened cable. **In the case of a screened cable, there are additional transversal impedance cells between each single conductor and the screen.** As in the longitudinal and transversal impedance model, if one wants to increase the bandwidth of the cell model, more R-L or R-C branches can be added to the longitudinal and transversal impedances.

2.4 Cell model of a two-conductor screened cable including the longitudinal and transversal impedances

In the case of a two-conductor screened cable, there is also a capacitive coupling between the screen and the two conductors, which is illustrated in the next figure. To obtain the longitudinal and transversal cable parameters four tests have to be performed, that is, two circuit tests and two open circuit tests under common mode and differential mode connection.

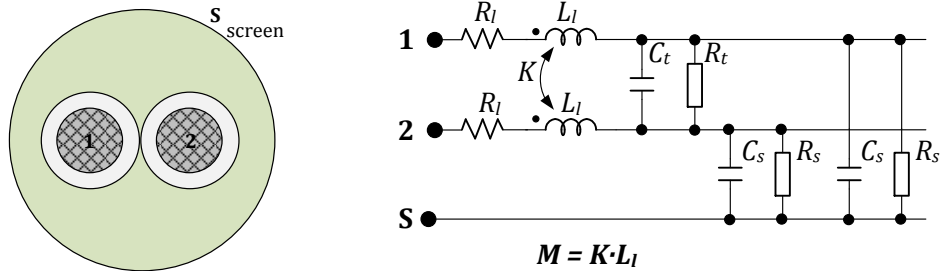


Fig. 2.4. Cell model for a two-conductor screened cable.

2.5 Cell model of an three-conductor unscreened cable including the longitudinal and transversal impedances

In this model, since there is not a screen, only the inductive and capacitive couplings between conductors are considered. To determine the cable parameters two tests must be performed, that is, the short circuit and open circuit tests.

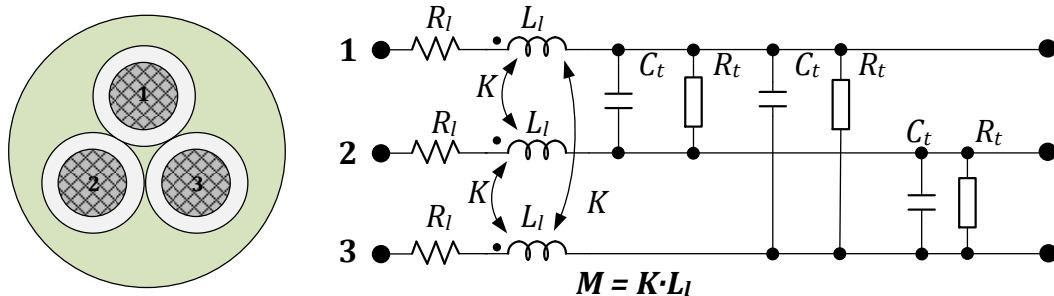


Fig. 2.5. Cell model for a three-conductor unscreened cable.

2.6 Cell model of a three-conductor screened cable including the longitudinal and transversal impedances

In this model, since there is a screen, the capacitive couplings between the conductors and the screen are considered. To determine the cable parameters four tests must be performed, two the short circuit and two open circuit tests.

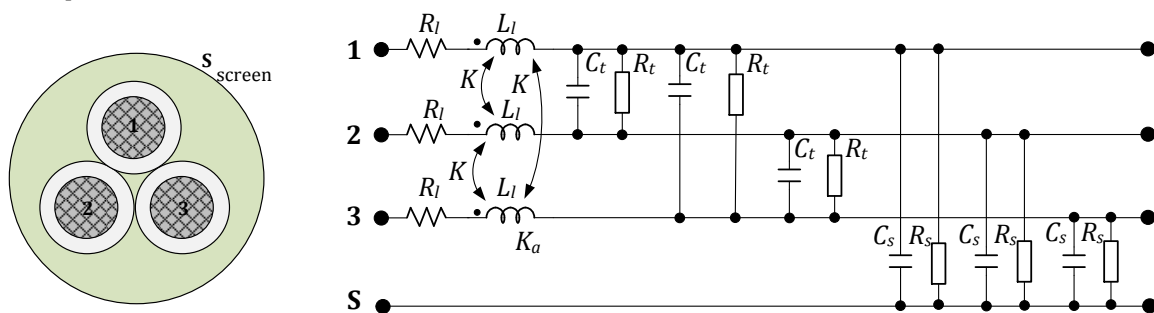


Fig. 2.6. Cell model for a three-conductor screened cable



MULTYCAB

February 2015 Deliverables 2

Document	Deliverable 2
Facilities	-
Revision	Revised
Date	February 2015

Experimental measurements



3 Experimental setup and cable parameters determination

In this section the experimental setup to determine the frequency response of a multi-conductor cable as well as the determination of the cable parameters to develop a broad-frequency model of the multi-conductor cable is described.

3.1 The impedance analyzer to conduct the experimental tests

To measure the frequency response of the cable a wide-band high-precision impedance analyzer will be used.

It allows measuring parameters such as:

- $|Z|-\theta, R-X,$
- $L_s-R_s, C_s-R_s,$
- $|Y|-\theta, G-B, L_p-G,$
- $L_p-Q, C_p-G,$
- L_p-R_p, C_p-R_p
- Frequency range: 40 Hz - 110 MHz, resolution 1 mHz
- Voltage Signal Level Range: 5 mVrms - 1 Vrms , resolution 1 mV
- Current Signal Level Range: 200 μ Arms to 20 mArms, resolution 20 μ A

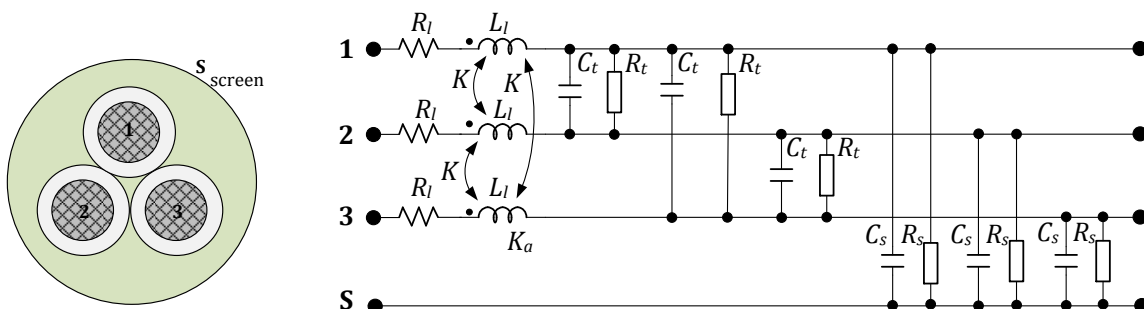
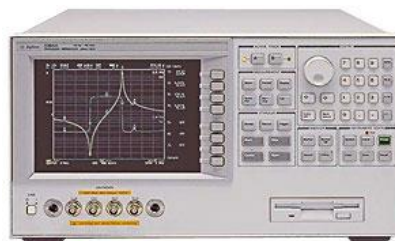


Fig. 3.1. Agilent 4294A impedance analyzer and cable parameters to be determined

To determine the parameters of the cell shown in Fig. 3.1 different experimental tests must be performed, as detailed in the following subsections.

It is worth noting that the longitudinal parameters (R_l, X_l, K) are found through short circuit tests, whereas the transversal parameters ($C_t, G_t = 1/R_t, C_s, G_s = 1/R_s$) are found by applying open circuit tests.

All tests are performed at a pre-established frequency, for example, 500 kHz.

3.2 Experimental measurement of the model parameters of a two-conductors unshielded cable

To determine the cable parameters two tests should be performed, that is, the short circuit and the open circuit tests, as detailed in the following subsections.

In a two-conductor unshielded cable it is not necessary to take into account the mutual coupling coefficient between the inductances of conductors 1 and 2 since it is possible to group terms L_f and M because $I_2 = -I_1$,

$$U_1 = L_1 \frac{dI_1}{dt} + M \frac{dI_2}{dt} = L_1 \frac{dI_1}{dt} - M \frac{dI_1}{dt} = (L_1 - M) \frac{dI_1}{dt} = L \frac{dI_1}{dt}$$

Similarly,

$$U_2 = L_1 \frac{dI_2}{dt} + M \frac{dI_1}{dt} = L_1 \frac{dI_2}{dt} - M \frac{dI_2}{dt} = (L_1 - M) \frac{dI_2}{dt} = L \frac{dI_2}{dt}$$

Where $M = K \cdot L_1$, K being the coupling coefficient between conductors 1 and 2.

Next figure shows the geometry of the cable,

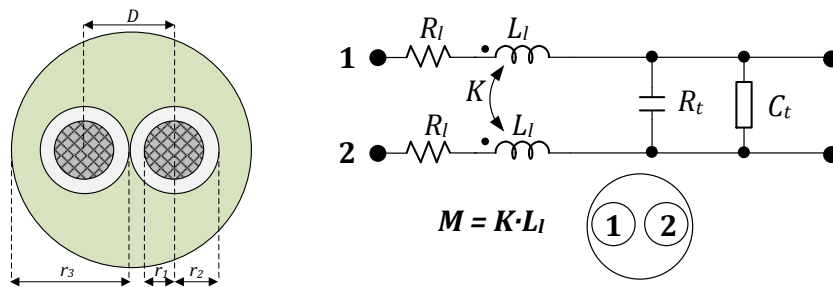


Fig. 3.2 Geometry of the two-conductors unshielded cable and full cell model of the cable

As shown in Fig. 3.2 there are four parameters to determine, that is, R_l , $L = L_1 - M$, G_t and C_t . This is done by means of two tests, the short circuit and open circuit tests.

3.2.1 Short circuit test in a two-conductors unshielded cable

In this test two conductors are short circuited as detailed in the following figure. The short circuit test allows determining the longitudinal cable parameters.

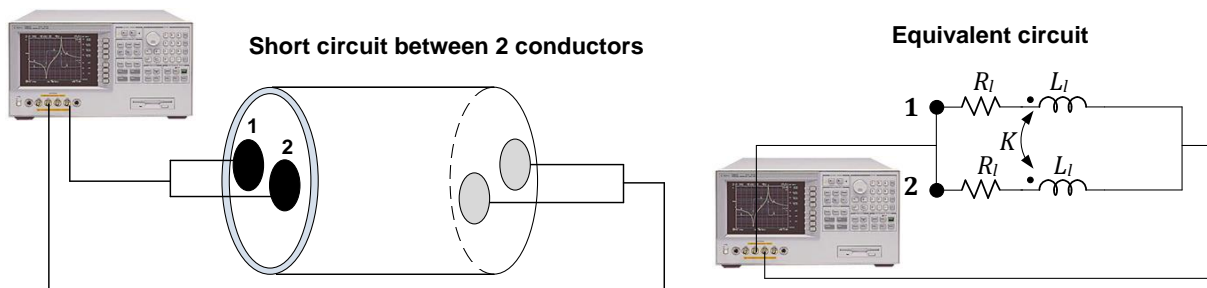


Fig. 3.3. Setup to measure the short circuit between two adjacent conductors

From the reading of the impedance analyzer it results [Moureau_Thesis],

$$L_{measured} = \frac{L}{2}$$

$$R_{measured} = \frac{R_l}{2}$$

where $L = L_1 - M$.

It is also possible to determine the longitudinal parameters by applying the following formulas which take into account the skin effect [WeensThesis],

$$R_l = \rho \frac{1}{\pi \left[r_1^2 - \left(r_1 - \frac{1}{(\pi f \mu \sigma)^{1/2}} \right)^2 \right]} \quad [\text{Ohm/m}]$$

$$L = \frac{10^{-4}}{2r_1 \sqrt{1 - (2r_1/D)^2}} \sqrt{\frac{\mu_r}{\sigma f}} + 2 \cdot 10^{-7} \ln \left[\frac{D}{2r_1} (1 + \sqrt{1 - (2r_1/D)^2}) \right] \quad [\text{H/m}]$$

3.2.2 Open circuit test in a two-conductors unscreened cable

In this test the two conductors are in open circuit as detailed in the following figure. The open circuit test allows determining the transversal cable parameters.

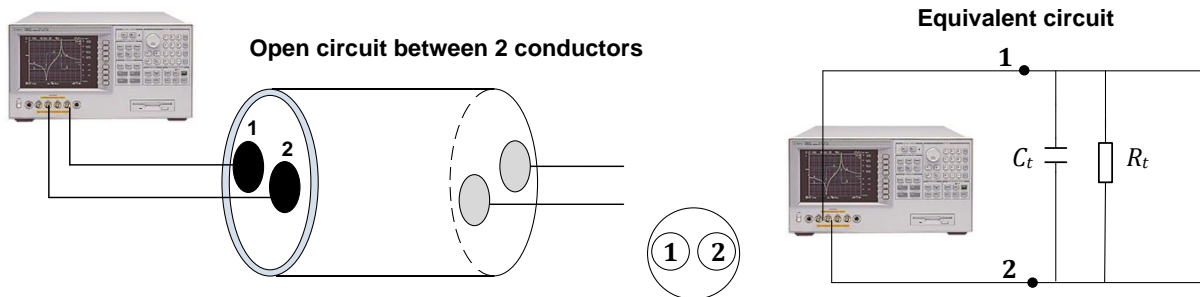


Fig. 3.4. Setup to measure the open circuit between two adjacent conductors and equivalent circuit

From the reading of the impedance analyzer it results [Moureau_Thesis],

$$C_{measured} = C_t$$

$$G_{measured} = G_t = 1/R_t$$

It is also possible to determine the transversal parameters by applying the following formulas [WeensThesis],

$$C_t = \frac{\pi \epsilon_0 \epsilon_r}{\ln \left(\frac{D - r_1}{r_1} \right)} \quad [\text{F/m}]$$

$$G_t = \frac{1}{R_t} = 2\pi f C_t \tan \delta \quad [\text{S/m}]$$

Where $\tan \delta = 44 \cdot 10^{-3}$ at 500 kHz for PVC

3.3 Experimental measurement of the model parameters of a three-conductors unscreened cable

To determine the cable parameters two tests should be performed, that is, the short circuit and the open circuit tests, as detailed in the following subsections.

In a three-conductor unscreened cable it is not necessary to take into account the mutual coupling coefficient between the inductances of conductors 1, 2 and 3 since it is possible to group terms L_f and M because $I_2 + I_3 = -I_1$,

$$U_1 = L_1 \frac{dI_1}{dt} + M \frac{dI_2}{dt} + M \frac{dI_3}{dt} = L_1 \frac{dI_1}{dt} + M \frac{d(I_2 + I_3)}{dt} = L_1 \frac{dI_1}{dt} - M \frac{dI_1}{dt} = (L_1 - M) \frac{dI_1}{dt} = L \frac{dI_1}{dt}$$

Where $M = K \cdot L_1$, K being the coupling coefficient between two conductors.

Next figure shows the geometry of the cable,

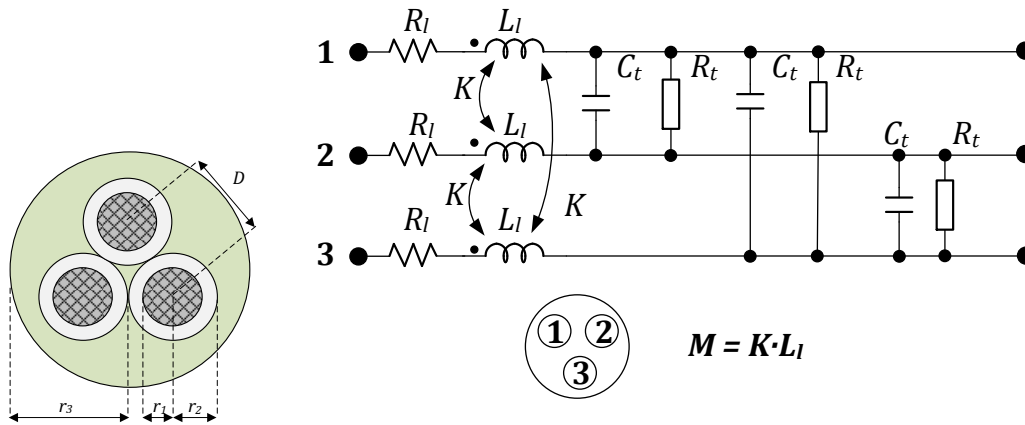


Fig. 3.5 Geometry of the three-conductor unscreened cable and full cell model of the cable

As shown in Fig. 3.5 there are four parameters to determine, that is, R_l , $L = L_l - M$, G_t and C_t . This is done by means of two tests, the short circuit and open circuit tests.

3.3.1 Short circuit test in a three-conductor unscreened cable

In this test two conductors are short circuited as detailed in the following figure. The short circuit test allows determining the longitudinal cable parameters.

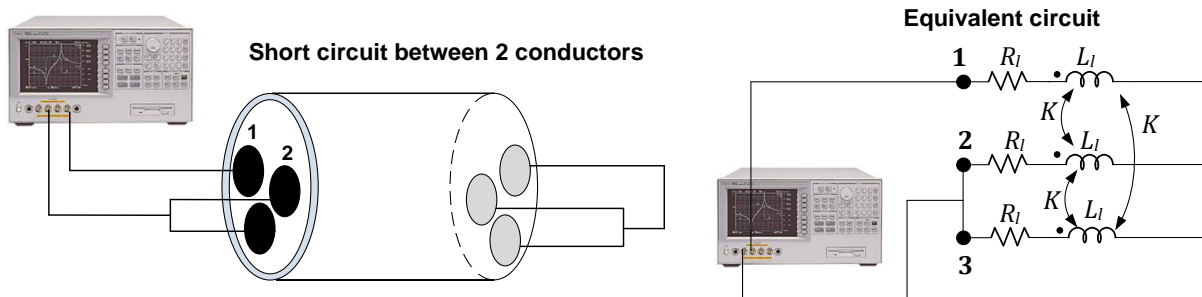


Fig. 3.6. Setup to perform the short circuit test and equivalent circuit

From the reading of the impedance analyzer it results [Moureau_Thesis],

$$L_{measured} = \frac{3L}{2}$$

$$R_{measured} = \frac{3R_l}{2}$$

where $L = L_l - M$.

It is also possible to determine the longitudinal parameters by applying the following formulas which take into account the skin effect [WeensThesis],

$$R_l = \rho \frac{1}{\pi \left[r_1^2 - \left(r_1 - \frac{1}{(\pi f \mu \sigma)^{1/2}} \right)^2 \right]} \quad [\text{Ohm/m}]$$

$$L = \frac{\mu}{2\pi} \ln\left(\frac{D^2}{r_1^2}\right) \quad [\text{H/m}]$$

3.3.2 Open circuit between test in a three-conductors unscreened cable

In this test the three conductors are in open circuit as detailed in the following figure. The open circuit test allows determining the transversal cable parameters.

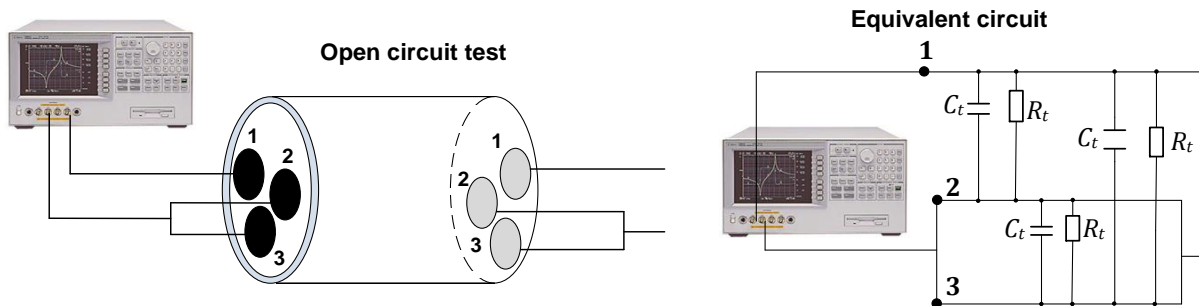


Fig. 3.7. Setup to perform the open circuit test and equivalent circuit

From the reading of the impedance analyzer it results [Moureau_Thesis],

$$C_{measured} = 2C_t$$

$$G_{measured} = 2G_t$$

It is also possible to determine the transversal parameters by applying the following formulas [WeensThesis],

$$C_t = \frac{\frac{\mu_0}{2\pi} \ln(D^2 / r_1^2)}{\frac{1}{\mu\epsilon} \left[\left[\frac{\mu_0}{2\pi} \ln(D^2 / r_1^2) \right]^2 - \left[\frac{\mu_0}{2\pi} \ln(D / r_1) \right]^2 \right]} \quad [\text{F/m}]$$

$$G_t = \frac{1}{R_t} = 2\pi f C_t \tan \delta \quad [\text{S/m}]$$

Where $\tan \delta = 44 \cdot 10^{-3}$ at 500 kHz

3.4 Experimental measurement of the model parameters of a two-conductors screened cable

To determine the cable parameters two tests should be performed, that is, the short circuit and the open circuit tests, as detailed in the following subsections.

In a two-conductor screened cable, there is a non-zero current flowing through the screen, so it is no longer possible to group terms L_f and M as done when dealing with unscreened cables, so the cable must be characterized by the inductance L_l of each driver and the coupling coefficient $K = M/L_l$,

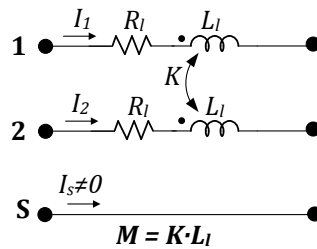


Fig. 3.9. Longitudinal equivalent circuit of the two-conductors screened cable

In this circuit, for conductor 1 it results,

$$U_1 = L_l \frac{dI_1}{dt} + M \frac{dI_2}{dt} = L_l \frac{dI_1}{dt} + KL_l \frac{dI_2}{dt}$$

For each configuration, short circuit and an open circuit tests should be performed. The measures in the common mode configuration are performed without *balun* (balanced-unbalanced lines transformer) since the measurement configuration adopted is asymmetric. However, the *balun* is required for measurements in the differential mode. For these tests, the different cable parameters are determined at a frequency of 500 kHz.

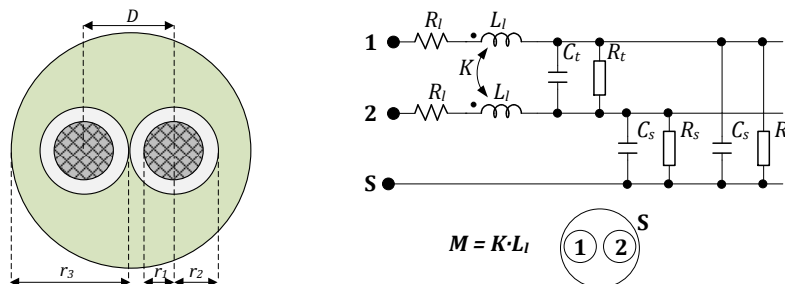


Fig. 3.10 Geometry of the two-conductors screened cable and full cell model of the cable

As shown in Fig. 3.10 there are seven parameters to determine, that is, R_l , L_l , K , G_t , C_t , G_s and C_s . This is done by means of four tests, that is, two short circuit tests (common mode CM and differential mode DM) and two open circuit tests (common mode CM and differential mode DM).

3.4.1 Short circuit tests in a two-conductors screened cable (CM and DM)

In these tests two conductors are short circuited as detailed in the following figure. The short circuit test allows determining the longitudinal cable parameters.

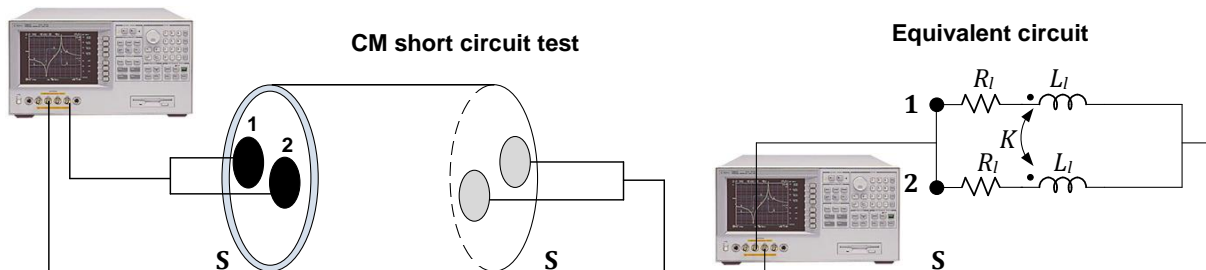


Fig. 3.11. Common mode setup to perform the short circuit test and equivalent circuit

In a this case, since $I_1 = I_2$ it results,

$$U_1 = L_l \frac{dI_1}{dt} + M \frac{dI_2}{dt} = L_l \frac{dI_1}{dt} + M \frac{dI_1}{dt} = (L_l + M) \frac{dI_1}{dt}$$

Therefore, from the reading of the impedance analyzer it results [Moureau_Thesis],

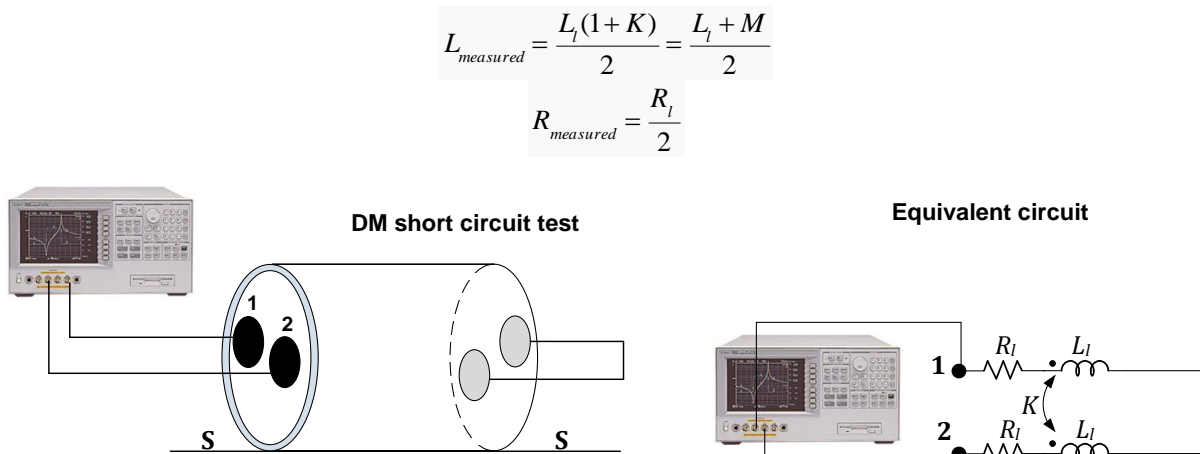


Fig. 3.12. Differential mode setup to perform the short circuit test and equivalent circuit

In a this case, since $I_1 = -I_2$ it results,

$$U_1 = L_l \frac{dI_1}{dt} + M \frac{dI_2}{dt} = L_l \frac{dI_1}{dt} - M \frac{dI_1}{dt} = (L_l - M) \frac{dI_1}{dt}$$

Therefore, from the reading of the impedance analyzer it results [Moureau_Thesis],

$$L_{measured} = 2L_l(1 - K) = 2(L_l - M)$$

$$R_{measured} = 2R_l$$

3.4.2 Open circuit between test in a two-conductors screened cable (CM and DM)

In these tests the two conductors are in open circuit as detailed in the following figure. The open circuit tests allow determining the transversal cable parameters.

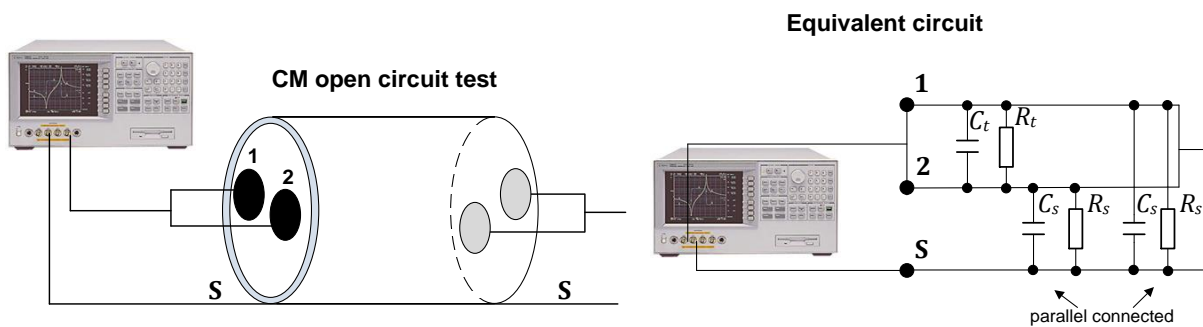


Fig. 3.13. Common mode open circuit test and equivalent circuit

From the reading of the impedance analyzer it results [Moureau_Thesis],

$$C_{measured} = 2C_s$$

$$G_{measured} = 2G_s$$

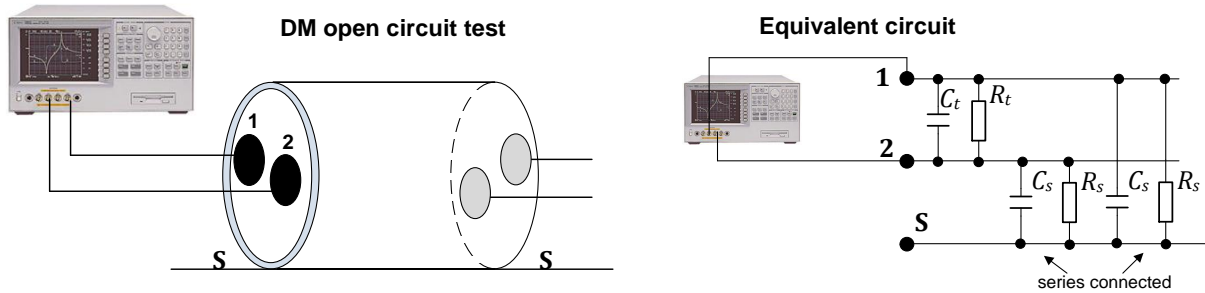


Fig. 3.13. Differential mode open circuit test and equivalent circuit

From the reading of the impedance analyzer it results [Moureau_Thesis],

$$C_{measured} = C_t + C_s / 2$$

$$G_{measured} = G_t + G_s / 2$$

3.5 Experimental measurement of the model parameters of a 3-conductors screened cable

To determine the parameters four tests should be performed, that is, two short circuit tests with 2 or 3 conductors in short circuit, and two open circuit tests, with 2 or 3 conductors in open circuit as detailed in the following subsections.

3.5.1 Short circuit tests

In this test two or three adjacent conductors are short circuited as detailed in the following figure. The short circuit test allows determining the longitudinal cable parameters.

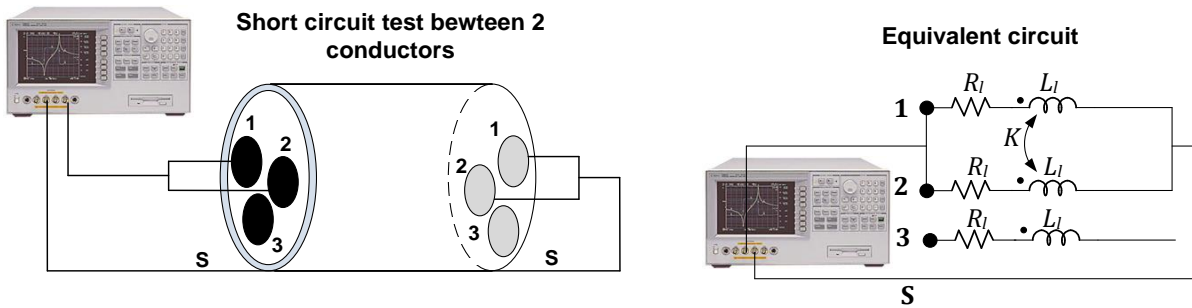


Fig. 3.14. Setup to perform the short circuit between two conductors

In this case, since $I_2 = I_1$, it results in,

$$U = I_1 R_i + L_i \frac{dI_1}{dt} + M \frac{dI_2}{dt} = I_1 R_i + L_i \frac{dI_1}{dt} + M \frac{dI_1}{dt} = I_1 R_i + (L_i + M) \frac{dI_1}{dt}$$

From the reading of the impedance analyzer it results [Moureau_Thesis],

$$L_{measured} = \frac{L_i(1+K)}{2} = \frac{L_i + M}{2}$$

$$R_{measured} = \frac{R_i}{2}$$

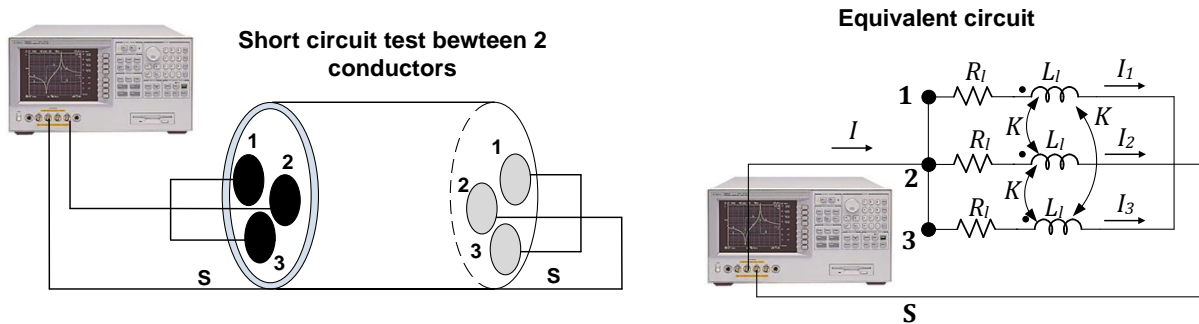


Fig. 3.15. Setup to perform the short circuit between three conductors

In this case, since $I = I_1 + I_2 + I_3$ it results in,

$$U = I_1 R_l + L_l \frac{dI_1}{dt} + M \frac{dI_2}{dt} + M \frac{dI_3}{dt}$$

$$U = I_2 R_l + L_l \frac{dI_2}{dt} + M \frac{dI_1}{dt} + M \frac{dI_3}{dt}$$

$$U = I_3 R_l + L_l \frac{dI_3}{dt} + M \frac{dI_1}{dt} + M \frac{dI_2}{dt}$$

By adding the three equations above and taking into account $I = I_1 + I_2 + I_3$ it results,

$$3U = IR_l + L_l \frac{dI}{dt} + 2M \frac{dI}{dt} \rightarrow U = I \frac{R_l}{3} + \frac{L_l}{3} \frac{dI}{dt} + \frac{2M}{3} \frac{dI}{dt}$$

Therefore, from the reading of the impedance analyzer it results,

$$L_{measured} = \frac{L_l(1+2K)}{3} = \frac{L_l + 2M}{3}$$

$$R_{measured} = \frac{R_l}{3}$$

3.5.2 Open circuit tests

In these tests two or three conductors are in open circuit as detailed in the following figure. The open circuit test allows determining the transversal cable parameters.

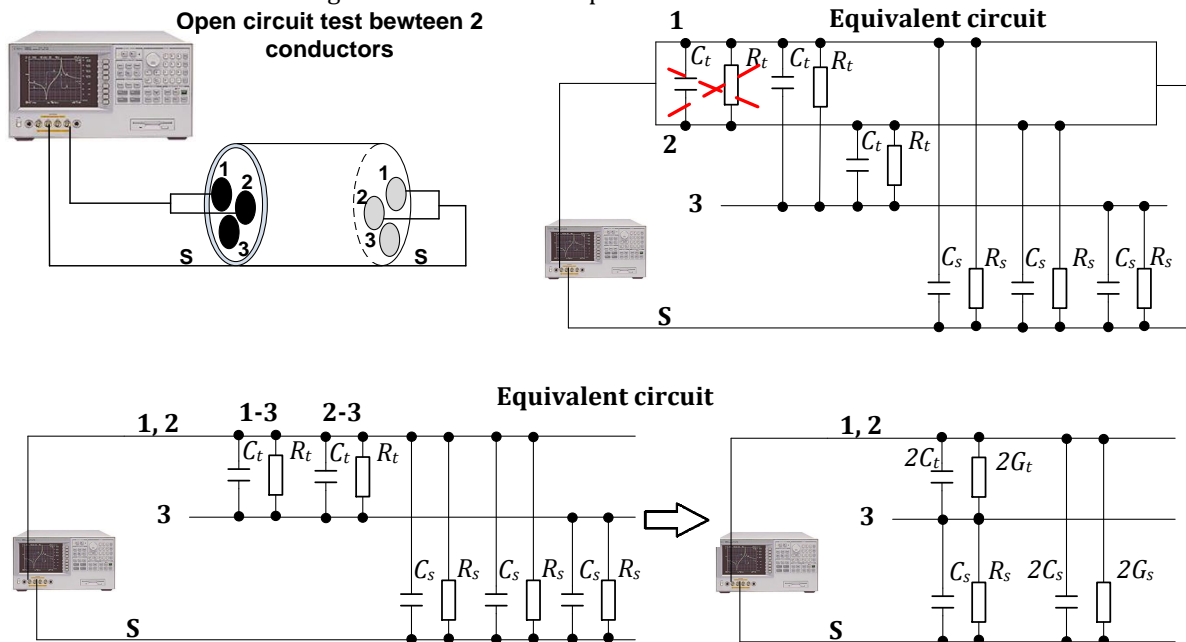


Fig. 3.16. Setup to perform the open circuit test between two conductors and equivalent circuit

From this circuit it results,

$$C_{measured} = \frac{2C_t \cdot C_s}{2C_t + C_s} + 2C_s$$

$$G_{measured} = \frac{2G_t \cdot G_s}{2G_t + G_s} + 2G_s$$

Where $G_t = 1/R_t$, $G_s = 1/R_s$.

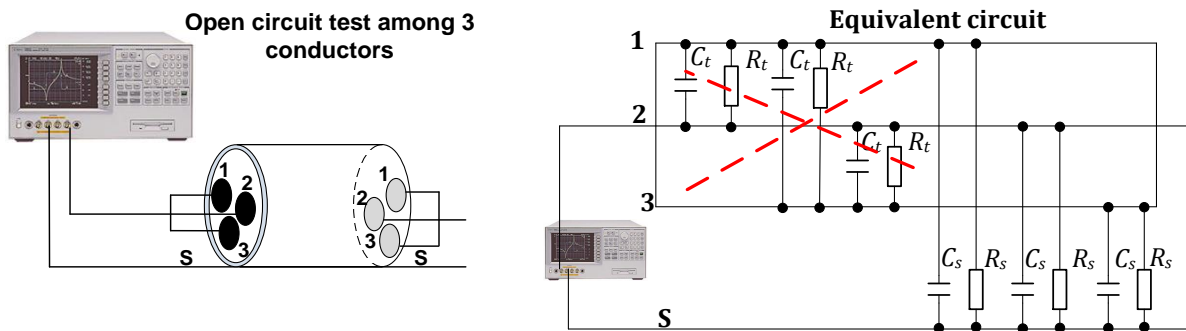


Fig. 3.17. Setup to perform the open circuit test between three conductors and equivalent circuit

From this circuit, since the capacitances and conductances between conductors 1,2,3 and the screen are in parallel it results,

$$C_{measured} = 3C_s$$

$$G_{measured} = 3G_s$$

Where $G_t = 1/R_t$, $G_s = 1/R_s$.

3.6 Model parameters in the range 40 Hz- 40 MHz

The purpose of this part is to determine the cable circuit model of any of the configurations analyzed in the sections above (two-conductors screened or unscreened or three-conductor screened or unscreened) valid for a frequency band 40 Hz - 40MHz.

For this, it is possible to model the evolution of the parameters of the linear function of the frequency cable with ladder circuit networks. The objective is to determine the parameters of such ladder networks. But for this, we must first determine the evolution of the line parameters with the frequency. In the same manner as above, an experimental method using an impedance analyzer will be applied to selected cable configuration.

The principle of this method consists in measuring changes in the line parameter as a function of the frequency by using the impedance analyzer. Such as above, the short-circuit test will determine the evolution of resistance and inductance per unit length R_l and L_l as a function of the frequency, and the open circuit test will determine the evolution of different capacities and conductance per unit length. **In this case a 10cm cable sample is used.** The reason is explained in the following.

When using a longer cable, the resonance frequencies tend to occur at lower frequencies than in a shorter cable. For example in [Moureau_Thesis] it is shown that for a 5 meter cable, the first resonance peak appears at 8 MHz. Since the information extracted is only representative for frequencies below one-tenth of the first resonance frequency, the study of a 5 meter cable only provides reliable values up to 800 kHz. In the case of a 10 cm cable, the first resonance peak will be placed at approximately 400 MHz, so the study can be valid up to 40 MHz. Therefore, in order to extend this frequency range, a short conductor must be analyzed. For this reason a 10 cm cable is selected.

The evolution of the cable parameters according to the frequency is determined from a 10 cm cable sample. If, for example, a three-conductor screened cable is analyzed, the short circuit and open circuit tests in the range 40 Hz – 40 MHz summarized in next figure can be carried out.

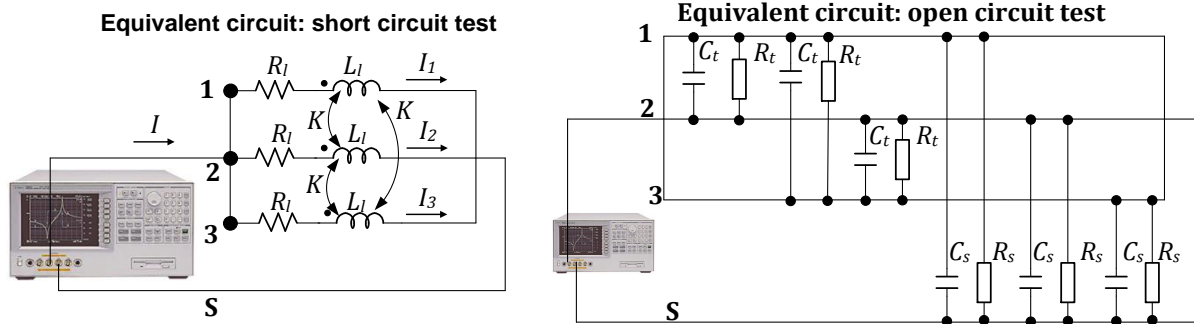


Fig. 3.18. Setup to measure : a) $R_{measured}$ and $L_{measured}$ b) $G_{measured}$ and $C_{measured}$

Note that for this particular case we have,

$$L_{measured} = \frac{L_l(1+2K)}{3} = \frac{L_l + 2M}{3}$$

$$R_{measured} = \frac{R_l}{3}$$

$$C_{measured} = 3C_s$$

$$G_{measured} = 3G_s$$

The following figure shows the evolution of the parameters $R_{measured}$, $L_{measured}$, $G_{measured}$ and $C_{measured}$ measured by the impedance analyzer in the range 40 Hz-40 MHz when using a 10 cm 3-conductors screened cable.

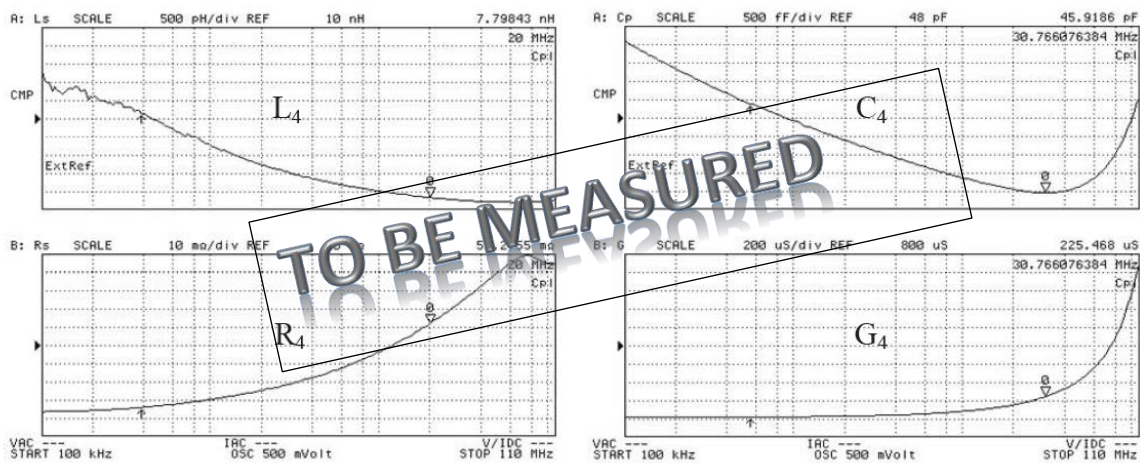


Fig. 3.19. Measured values of $R_{measured}$, $L_{measured}$, $G_{measured}$ and $C_{measured}$ in the 40 Hz - 40 MHz frequency interval.

1.- First hypothesis. The magnetic coupling coefficients K between conductors are considered constant, so it is supposed they do not vary with the frequency. The direct consequence of this assumption is that changes in inductance per unit length of a conductor as a function of the frequency is the same as the equivalent inductance $L_{measured}$. Therefore, by applying a dilation of the evolution of $L_{measured}$ measured over a 10 cm cable, it is easy to find the evolution of L_l for 1 meter cable as shown in Fig. 3.20. The reference value for L_l is the value determined at 500 kHz in the first part of this study.

2.- Second hypothesis. The evolution of the cross line capacitances (C_t) with the frequency is the same as the equivalent capacitance $C_{measured}$ measured during testing and C_s (capacitance per unit length between each conductor and the shield) has the same evolution as $C_{measured}$ ($C_{4,eq} = 3C_s$). Similarly, it is required to apply a dilation of the evolution of $C_{4,eq}$ measured 10cm cable to find the C_t and C_s values for a cable length of one meter. Reference values for C_t and C_s are those found in the 500 kHz measure.

Since the magnetic coupling coefficient K was calculated at 500 kHz, the evolution of the other cable parameters are directly obtained from the following figure.

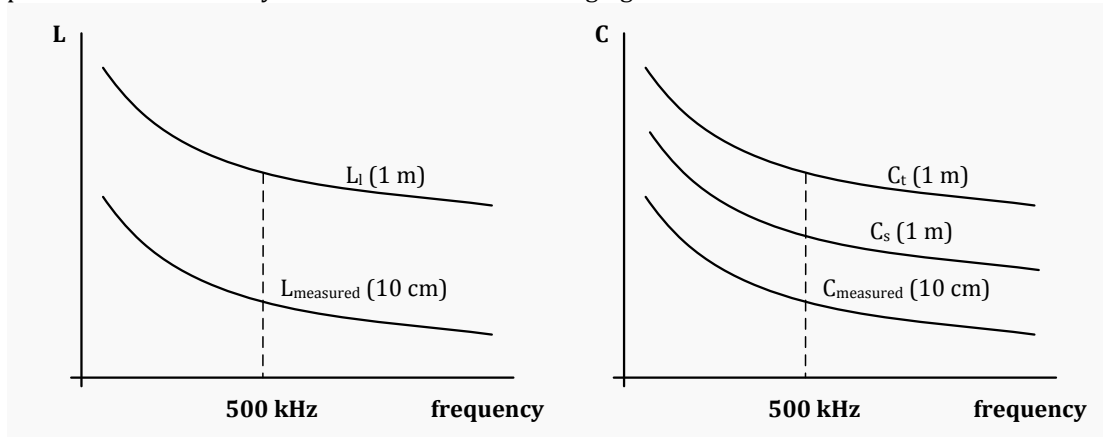


Fig. 3.20. Frequency dependence of inductances and capacitances.

The experimental method and its assumptions have been exposed, therefore now it is possible to model the behavior of the cable from different network scale circuits.



Document	Deliverable 2
Facilities	-
Revision	Revised
Date	February 2015

Cell parameters fitting by applying genetic algorithms

4 GA-based iterative algorithm to adjust the coefficients of the impedance network from the measured frequency response of the cable

In this section the method used to adjust the coefficient values (R and L or C values) of a given circuit to match its response with that measured with a wide-band impedance analyzer is explained.

The first step consists in measuring the frequency response of the cable by using a suitable wide-band impedance analyzer which provides the frequency response $R(f)$, $L(f)$ and $C(f)$ of the measured cable configuration.

Once the frequency response is obtained only some relevant points are retained to minimize the computational load of the next steps, since this is a complex problem demanding high computational requirements. This step is shown in Fig. 4.1, where the red dots are the only points used in the calculations.

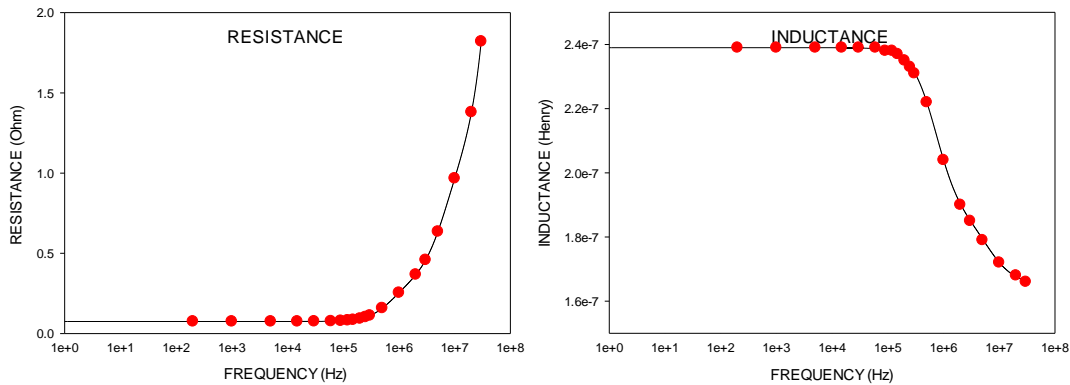


Fig. 4.1. Equivalent impedance as a function of the frequency of a) Equivalent resistance, R b) Equivalent inductance, L

The next step consists in selecting a suitable circuit which is supposed it can reproduce with fidelity the frequency response displayed in Fig. 1. This is a critical part, since there are a limited number of circuits which can match a determined frequency response, so the election of the suitable circuit is based in previous experiences obtained from the technical bibliography [ThesisMoureau,Weens]. We have selected for this particular frequency response the circuit shown in Fig. 2.

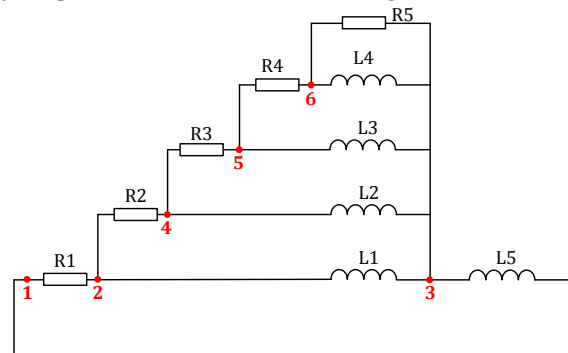


Fig. 4.2. Selected impedance to reproduce the frequency response shown in Fig. 4.1

Once the experimental frequency response of the impedance has been measured with the impedance analyzer and the circuit to reproduce this frequency response has been selected, the parameters R_i and L_i or C_i of the circuit must be adjusted in order to match the frequency response of the circuit with the experimental one.

Document	Deliverable 2
Facilities	-
Revision	Revised
Date	February 2015

To adjust the values of all the parameters in each cell of the high-frequency model, an iterative genetic algorithm (GA) is applied.

GAs are a family of mathematical methods which are founded in the concept of natural selection. Therefore the most suitable individuals are those which are more likely to survive, and the least fitted solution individuals have a reduced reproduction probability. GAs perform an iterative heuristic search which randomly selects a set of individuals from the current population at each step. After some generations the solution tends to an optimum, it usually minimizes the objective function. The individuals producing a local optimal are selected at each step and taken as the parents of the off individual springs for the next generation. This process is repeated, thus producing a population of individuals evolving toward an optimal solution.

GAs apply mathematical operations which try to imitate genetic reproduction mechanisms. These operations include:

- **Individual's selection.** This operation selects the parents for the next generation
- **Crossover.** This operation combines two parents' solutions to produce offspring solutions for the next generation
- **Mutation.** This operation applies random changes to parents and children solutions to obtain an optimal solution.

In the problem under study there are several parameters (R_i and L_i with $i = 1, \dots, 5$ in the former example). These parameters are coded into binary strings forming the chromosomes. The elitist scattered crossover operation is applied, which at each generation produces a random binary vector from which the genes of both parents are combined to form the offspring. Next, the mutation process is applied, by which the GA creates small random variations in each bit of the chromosomes, providing genetic diversity and enabling GA to search for wider spaces. The whole process is repeated until an established tolerance criterion is achieved.

However, after performing an exhaustive study, it was detected that model performance is maximized when applying the above-explained process in an iterative manner. Therefore the GA algorithm is applied iteratively until the error is less than a predetermined tolerance value. When operating in this way, the solution of each step is the seed value for the initial population of the next iteration.

Therefore, when dealing with circuit in Fig. 2, the 10 input GA variables are $R_1, \dots, R_5, L_1, \dots, L_5$. From these values the equivalent series resistance and inductance at each frequency $R(f)$ and $L(f)$ must be fitted to the experimental ones which have been provided by the wide-band frequency analyzer. Since the frequency analyzer provides $R(f)$ and $L(f)$ vectors with hundreds of components, it is necessary to reduce the size of these vectors to a reduced number of components. In this work it was found 20 as a number satisfying both results accuracy and limited computational burden. Therefore, the objective function (ϵ) to be minimized is defined as the squared error between the 20 retained measured points ($R_{\text{measured},i}, L_{\text{measured},i}$) and the ones outputted by the GA algorithm ($R_{\text{calculated},i}, L_{\text{calculated},i}$)

$$\epsilon = \sum_{i=1}^{20} (R_{\text{calculated},i}/R_{\text{measured},i} - 1)^2 + (X_{\text{calculated},i}/X_{\text{measured},i} - 1)^2$$

where $X = 2\pi fL$

The adjustment of these parameters ($R_1, \dots, R_5, L_1, \dots, L_5$) is done by using an iterative genetic algorithm, as shown in the diagram in Fig. 3.

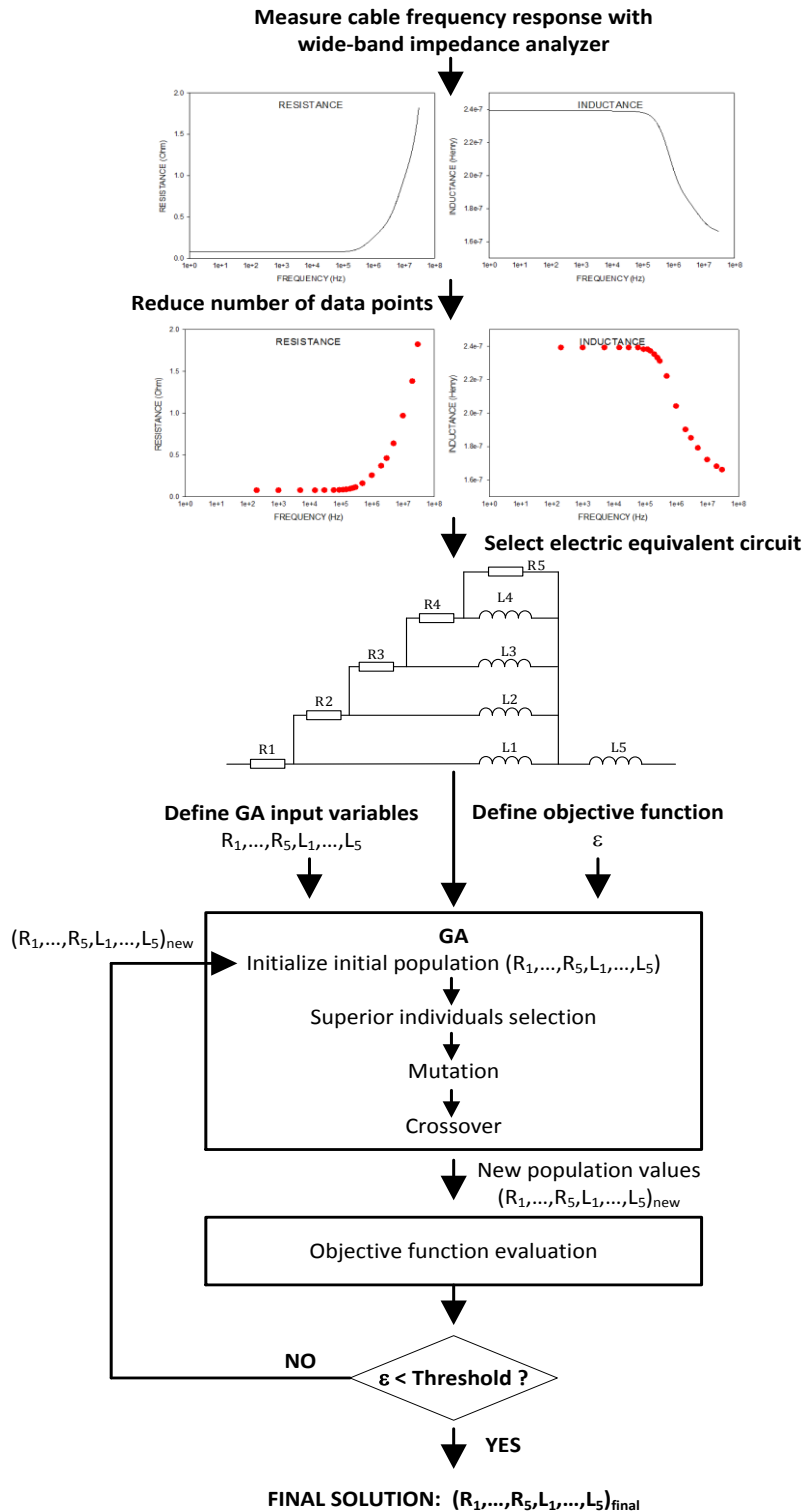


Fig. 4.3. Procedure to adjust the parameters ($R_1, \dots, R_5, L_1, \dots, L_5$)

Sometimes the procedure described in Fig. 4.3 fails to reach convergence because the electric equivalent circuit selected to model the frequency response cannot describe such a response. In this case additional branches must be added to such a circuit and repeat the full process described in Fig. 4.3.

4.1 Modelling the longitudinal impedance of an isolated conductor

In this section the components' values of the longitudinal impedance of a conductor are adjusted from the experimental frequency response. So, it is assumed we already have tested the conductor with a wide-band impedance analyzer in the range 40 Hz – 40 MHz.

Fig. 4.4 shows the frequency response of the longitudinal impedance R-L of the analyzed conductor as measured by the impedance analyzer.

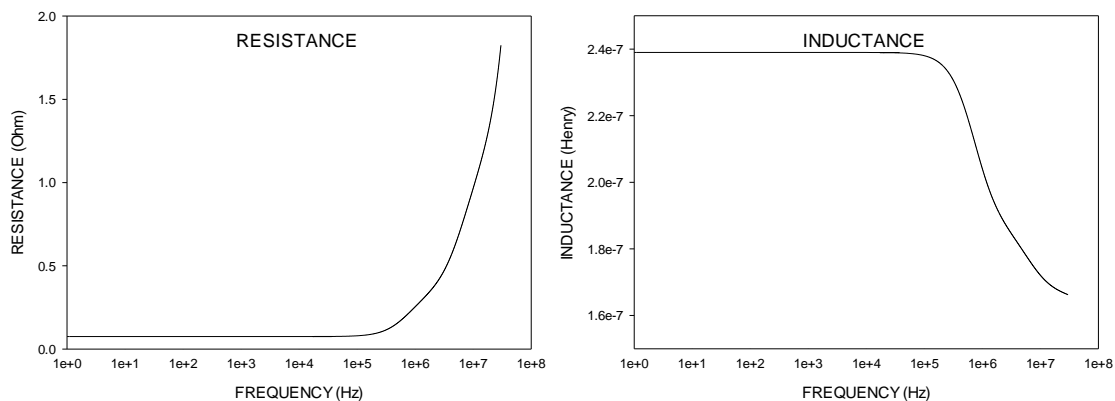


Fig. 4.4. Longitudinal impedance. Frequency evolution of a) Resistance, R b) Inductance, L

Let's assume that the circuit in Fig. 4.5 can reproduce the frequency response shown in Fig. 1 once the five resistances and the five inductances have been properly tuned.

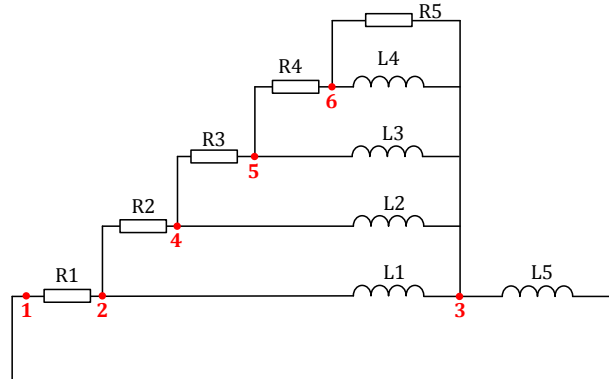


Fig. 4.5. Longitudinal impedance circuit model.

To determine the frequency response of circuit in Fig. 4.5 it is necessary to calculate the overall equivalent impedance of such a circuit as a function of the frequency. This goal can be achieved with the following code:

```
w=2*pi*f;
X1=w*L1; X2=w*L2; X3=w*L3; X4=w*L4; X5=w*L5;
%Calculation of Z1=A1+B1*i (real and imaginary parts) It includes R5, R4 and L4
A1=R4+(R5*X4^2)/(R5^2+X4^2); B1=R5*R5*X4/(R5^2+X4^2);
% Calculation of Z2=A2+B2*i It includes R5, R4, R3, L4, and L3
A2=R3+(A1*X3*(B1+X3)-A1*B1*X3)/(A1^2+(B1+X3)^2);
B2=(A1*A1*X3+B1*X3*(B1+X3))/(A1^2+(B1+X3)^2);
% Calculation of Z3=A3+B3*I It includes R5, R4, R3, R2, L4, L3 and L2
A3=R2+(A2*X2*(B2+X2)-A2*B2*X2)/(A2^2+(B2+X2)^2);
B3=(A2*A2*X2+B2*X2*(B2+X2))/(A2^2+(B2+X2)^2);
% Calculation of Z4=A4+B4*i It includes R5, R4, R3, R2, R1, L4, L3, L2 and L1
A4=R1+(A3*X1*(B3+X1)-A3*B3*X1)/(A3^2+(B3+X1)^2);
B4=(A3*A3*X1+B3*X1*(B3+X1))/(A3^2+(B3+X1)^2)+X5;
%Overall equivalent impedance:
Rcal=A4;
Xcal=B4;
```

Document	Deliverable 2
Facilities	-
Revision	Revised
Date	February 2015

Next, the values of R1, R2, R3, R4, R5, L1, L2, L3, L4 and L5 must be adjusted by applying the recursive GA method explained in Section 4, thus applying:

```
%Lower and upper bounds of R1, R2, R3, R4, R5, L1, L2, L3, L4 and L5
lb=[1e-2 1e-2 1e-2 1e-2 1e-2 1e-8 1e-8 1e-8 1e-8 1e-8];
ub=[0.2 1 3 8 20 2e-7 2e-7 2e-7 2e-7 2e-7];
```

```
%Seeds for initial population
InitialPopulation_Data=[0.05 0.1 0.5 1 2 1e-08 1e-08 1e-08 1e-08 1e-07];
```

Finally, the values of R1, R2, R3, R4, R5, L1, L2, L3, L4 and L5 obtained through the recursive GA method are as follows:

```
%Valued obtained by applying the recursive GA method:
R1 = 0.0749589805316786
R2 = 0.644241909383684
R3 = 2.21128763093572
R4 = 7.99999999002703
R5 = 0.939998646698948
L1 = 8.85613914295851e-08
L2 = 4.77644039744681e-08
L3 = 2.39517568049594e-08
L4 = 1.96917854657664e-07
L5 = 1.50058385970163e-07
```

The frequency response of the circuit in Fig. 4.5 with the resistances and inductances values obtained by applying the recursive GA method are plotted and compared with experimental data in Fig. 4.6. From these results one can see the close match between experimental data and circuit model of the longitudinal conductor impedance.

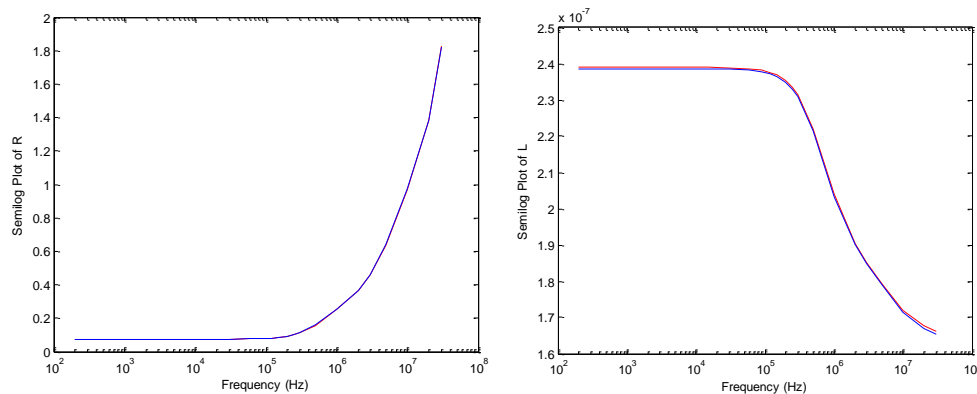


Fig. 4.6. Longitudinal impedance. Experimental values and predicted by the model.

4.2 Modelling the transversal impedance of an isolated conductor

In this section the components' values of the transversal impedance of a conductor are adjusted from the experimental frequency response. So, it is assumed we already have tested the conductor with a wide-band impedance analyzer in the range 40 Hz – 40 MHz.

Fig. 4.7 shows the frequency response of the longitudinal impedance G-C of the analyzed conductor as measured by the impedance analyzer.

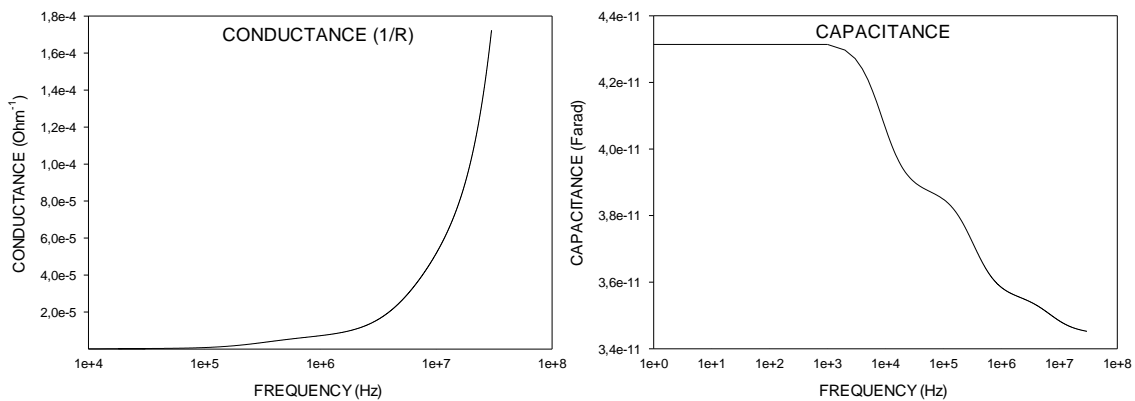


Fig. 4.7. Transversal impedance. Frequency evolution of a) Resistance, R b) Inductance, L

Let's assume that the circuit in Fig. 4.8 can reproduce the frequency response shown in Fig. 4.7 once the six resistances and the six capacitances have been properly tuned.

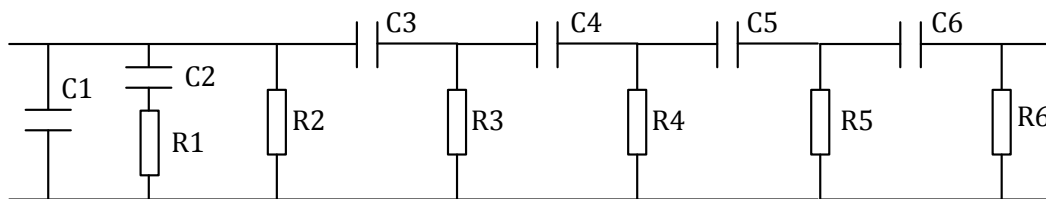


Fig. 4.8. Transversal impedance circuit model.

To determine the frequency response of circuit in Fig. 4.8 it is necessary to calculate the overall equivalent impedance of such a circuit as a function of the frequency. This goal can be achieved with the following code:

```
w=2*pi*f;
X1=-1/(w*C1); X2=-1/(w*C2); X3=-1/(w*C3); X4=-1/(w*C4); X5=-1/(w*C5); X6=-1/(w*C6);
%Calculation of Z6=A6+B6*i It includes R6 and C6
A6=R6; B6=X6;
% Calculation of Z5=A5+B5*i It includes R6, R5, C6 and C5
A5=R5*(A6*R5+A6^2+B6^2)/((R5+A6)^2+B6^2);
B5=X5+(B6*R5^2)/((R5+A6)^2+B6^2);
% Calculation of Z4=A4+B4*i It includes R6, R5, R4, C6, C5 and C4
A4=R4*(A5*R4+A5^2+B5^2)/((R4+A5)^2+B5^2);
B4=X4+(B5*R4^2)/((R4+A5)^2+B5^2);
% Calculation of Z3=A3+B3*i It includes R6, R5, R4, R3, C6, C5, C4 and C3
A3=R3*(A4*R3+A4^2+B4^2)/((R3+A4)^2+B4^2);
B3=X3+(B4*R3^2)/((R3+A4)^2+B4^2);
% Calculation of Z2=A2+B2*i It includes R6, R5, R4, R3, R2, C6, C5, C4 and C3
A2=((R2+A3)*R2*A3+R2*B3^2)/((R2+A3)^2+B3^2);
B2=(B3*R2^2)/((R2+A3)^2+B3^2);
% Calculation of Z1=A1+B1*i It includes R6, R5, R4, R3, R2, R1, C6, C5, C4, C3 and C2
A1=((A2*R1-X2*B2)*(A2+R1)+(A2*X2+R1*B2)*(X2+B2))/((R1+A2)^2+(X2+B2)^2);
B1=(-(X2+B2)*(A2*R1-X2*B2)+(A2*X2+R1*B2)*(R1+A2))/((R1+A2)^2+(X2+B2)^2);
% Calculation of Z0=A0+B0*I It includes R6, R5, R4, R3, R2,R1, C6, C5, C4, C3,C2 and C1
A0=(A1*X1^2)/(A1^2+(X1+B1)^2);
B0=(X1*A1^2+B1*X1*(X1+B1))/(A1^2+(X1+B1)^2);
```

Document	Deliverable 2
Facilities	-
Revision	Revised
Date	February 2015

```
%Calculation of parallel equivalent branch
```

```
Rcal=(A0^2+B0^2)/A0;
Xcal=(A0^2+B0^2)/B0;
```

Next, the values of R1, R2, R3, R4, R5, R6, C1, C2, C3, C4, C5 and C6 must be adjusted by applying the recursive GA method explained in Section 4, thus applying:

```
%Lower and upper bounds of R1, R2, R3, R4, R5, R6, C1, C2, C3, C4, C5 and C6
```

```
lb=[0 1 1 1 1 1 1e-13 1e-13 1e-13 1e-13 1e-13 1e-13];
ub=[1e8 1e8 1e8 1e8 1e7 1e7 1e-9 1e-9 1e-9 1e-9 1e-8 1e-8];
```

```
%Seeds for initial population
```

```
InitialPopulation_Data=[1 1e5 1e3 1e3 1e3 1e3 1e-10 1e-11 1e-10 1e-10 1e-10 1e-10];
```

Finally, the values of R1, R2, R3, R4, R5, R6, C1, C2, C3, C4, C5 and C6 obtained through the recursive GA method are as follows:

```
%Valued obtained by applying the recursive GA method:
```

```
R1=16.0396867812905
R2=99443124.7184383
R3=1271475.31934851
R4=4938826.05802273
R5=75328.2781539823
R6=11662.3938626871
C1=2.30629728905767e-11
C2=1.10874792662138e-11
C3=9.11627520407756e-12
C4=0.000999492421505371
C5=8.68723356844418e-12
C6=1.93267380873904e-12
```

The frequency response of the circuit in Fig. 4.8 with the resistances and inductances values obtained by applying the recursive GA method are plotted and compared with experimental data in Fig. 4.9. From these results one can see the close match between experimental data and circuit model of the longitudinal conductor impedance.

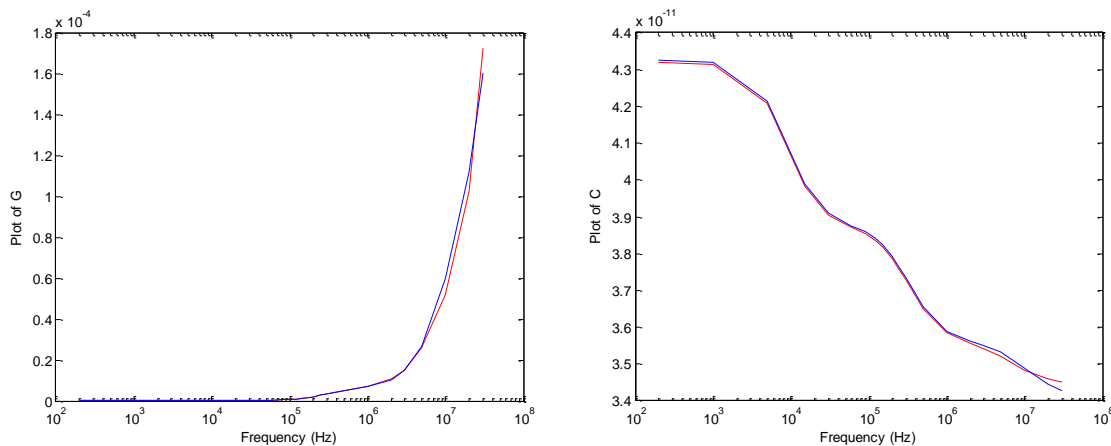


Fig. 4.9. Transversal impedance. Experimental values and predicted by the model.



MULTYCAB

February 2015 Deliverables 2

Document	Deliverable 2
Facilities	-
Revision	Revised
Date	February 2015

Transient circuit solver



5 R, L and C element models

In this section R, L and C element models are represented by a resistance in parallel with a current source (Norton representation) [Watson2007,EMTDC]. This system allows solving numerically the ordinary differential equations that explain the behavior of such elements by applying the trapezoidal integration rule or any other numerical implicit integration formula. It also allows converting the individual power system elements (R, L and C) into Norton equivalents, so the problem is easily solvable by applying nodal analysis.

Therefore the transient response of R, L and C elements will be calculated from an equivalent circuit formed by resistive branches and current sources. These resistors have constant values for a constant time step but the equivalent current sources are time and history dependent, whose values must be updated every time step.

In the Norton current source representation of each power system element, the Norton current source represents the component past or history, whereas the Norton impedance consists of a pure conductance element, which only depends on the time step length.

By choosing a suitable time integration step, this numerical integration strategy can be applied to any transient phenomena and to systems of any size. In some cases, however, the inherent truncation error of the trapezoidal method may lead to oscillations.

This structure allows to be processed by standard matrix methods, for example by applying the nodal analysis technique, in which a conductance matrix $|G|$ is formed from the inverse resistance value of each branch in the equivalent circuit. It is a square matrix, whose size is determined by the number of nodes in the analyzed circuit. A column matrix $|I|$ is formed where each element consists of the sum of all current sources at a node.

5.1 Trapezoidal rule of integration

The equivalent circuits of the inductor and capacitor, which are shown in Figs. 5.3 and 5.5, can be understood as a numerical representation of the governing ordinary differential equation, which are solved for discrete intervals. These equations for inductors and capacitors are integrated by using the trapezoidal rule since it is simple, fast, numerically stable, and accurate enough.

The trapezoidal integration rule can be summarized as in Fig. 5.1,

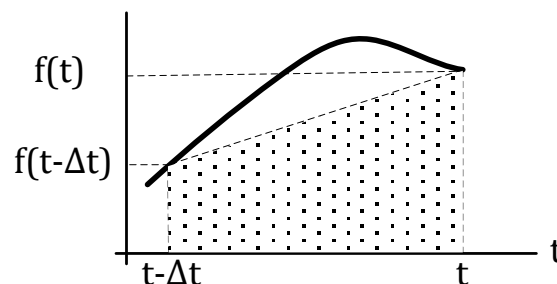


Fig. 5.1. Trapezoidal integration rule

The area enclosed between $t - \Delta t$ and t by applying the trapezoidal rule is as follows,

$$\int_{t-\Delta t}^t f(t) dt = \frac{\Delta t}{2} [f(t - \Delta t) + f(t)]$$

5.2 Resistance model

A resistor connected between nodes i and j can be represented by the equation:

$$u_i(t) - u_j(t) = i_{ij}(t) \cdot R \quad \rightarrow \quad i_{ij}(t) = \frac{u_i(t) - u_j(t)}{R} \quad (2)$$

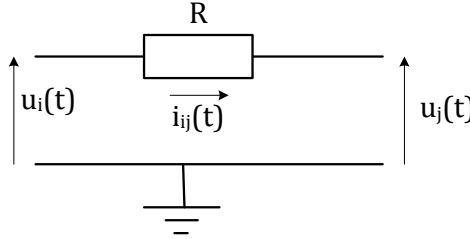


Fig. 5.2. Resistance representation

This formulation allows representing resistors accurately represented provided R is not too small. For very small values of R its inverse will be large, thus providing inaccurate results because of the finite precision of numerical calculations. On the other hand, very large values of R do not degrade the overall solution.

1.1 Inductance model

An inductor connected between nodes i and j can be represented by the differential equation:

$$u_i(t) - u_j(t) = L \cdot \frac{di_{ij}(t)}{dt} \quad (3)$$

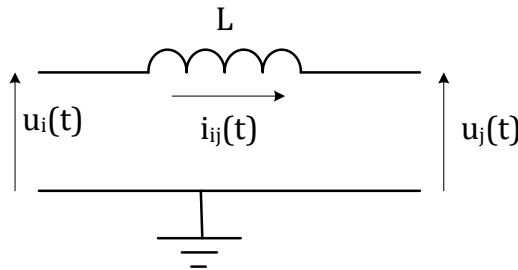


Fig. 5.3. Inductance representation

Eq. (3) can be solved as,

$$i_{ij}(t) = i_{ij}(t - \Delta t) + \frac{1}{L} \int_{t-\Delta t}^t [u_i(t) - u_j(t)] dt$$

By applying the trapezoidal integration rule it results in:

$$i_{ij}(t) = \underbrace{i_{ij}(t - \Delta t) + \frac{\Delta t}{2L} \cdot [u_i(t - \Delta t) - u_j(t - \Delta t)]}_{I_{history}(t-\Delta t)} + \underbrace{\frac{\Delta t}{2L}}_{1/R_{eff}} \cdot [u_i(t) - u_j(t)]$$

It results in,

$$i_{ij}(t) = I_{history}(t - \Delta t) + \frac{1}{R_{eff}} \cdot [u_i(t) - u_j(t)] \quad (4)$$

Where

$$R_{eff} = \frac{2L}{\Delta t}$$

$$I_{History}(t - \Delta t) = i_{ij}(t - \Delta t) + \frac{\Delta t}{2L} [u_i(t - \Delta t) - u_j(t - \Delta t)]$$

The analysis of inductors and capacitors in EMTDC is through their representation by a resistance in parallel with a current source as shown below:

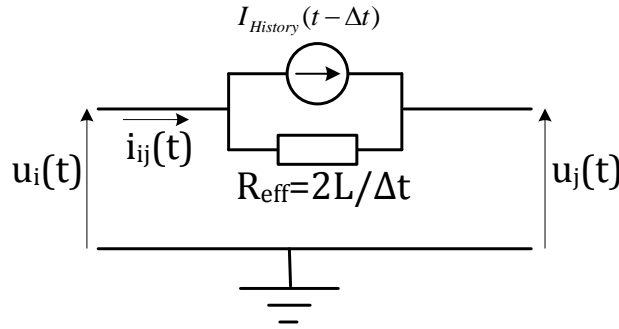


Fig.5. 4. Inductor representation

As occurred with the resistance, very small values of L or rather $2L/\Delta t$, can also result in poor conditioning of the conductance matrix thus leading to imprecise calculations.

5.3 Capacitance model

A capacitor connected between nodes i and j can be represented by the differential equation:

$$i_{ij}(t) = C \cdot d \frac{u_i(t) - u_j(t)}{dt} = C \cdot \frac{du_{ij}(t)}{dt} \quad (5)$$

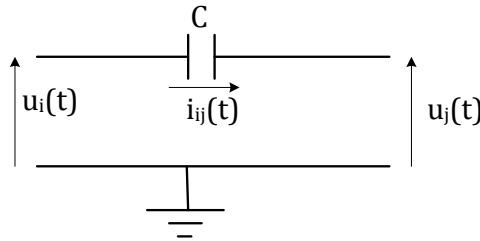


Fig. 5.5. Capacitor representation

Eq. (5) can be solved as,

$$u_{ij}(t) = u_i(t) - u_j(t) = u_{ij}(t - \Delta t) + \frac{1}{C} \int_{t-\Delta t}^t i_{ij}(t) dt$$

By applying the trapezoidal integration rule it results in:

$$u_{ij}(t) = u_{ij}(t - \Delta t) + \frac{\Delta t}{2C} i_{ij}(t - \Delta t) + \frac{\Delta t}{2C} i_{ij}(t)$$

It results in,

$$i_{ij}(t) = -i_{ij}(t - \Delta t) - \frac{2C}{\Delta t} u_{ij}(t - \Delta t) + \frac{2C}{\Delta t} u_{ij}(t)$$

$$i_{ij}(t) = I_{history}(t - \Delta t) + \frac{1}{R_{eff}} [u_i(t) - u_j(t)] \quad (6)$$

where

$$R_{eff} = \frac{\Delta t}{2C}$$

$$I_{History}(t - \Delta t) = -i_{ij}(t - \Delta t) - \frac{2C}{\Delta t} [u_i(t - \Delta t) - u_j(t - \Delta t)]$$

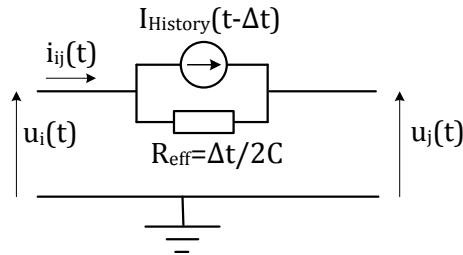


Fig. 5.6. Capacitor representation

If R_{eff} is too small, that is for large values of C (they are unlikely to be used), they can cause ill conditioning of the conductance matrix thus leading to numerical inaccuracy.

5.4 Integration results summary

The numerical integration in the previous sections is based on the trapezoidal integration rule. However, any other implicit formula of integration can be applied to derive the Norton equivalent circuit. Table I shows the Norton components resulting from different integration methods.

Table I. Norton equivalent circuit of elements for different integration methods

Integration method	Element	R_{eff}	$I_{History}$
Backward Euler		$L/\Delta t$	$i(t-\Delta t)$
Trapezoidal	Inductor	$2L/\Delta t$	$i_{ij}(t-\Delta t) + (\Delta t/2L) \cdot u_{ij}(t-\Delta t)$
Gear 2 nd order		$3L/(2\Delta t)$	$(4/3) \cdot i_{ij}(t-\Delta t) - (1/3) \cdot i_{ij}(t-2\Delta t)$
Backward Euler		$\Delta t/C$	$-(C/\Delta t) \cdot u_{ij}(t-\Delta t)$
Trapezoidal	Capacitor	$\Delta t/(2C)$	$-(2C/\Delta t) \cdot u_{ij}(t-\Delta t) - i_{ij}(t-\Delta t)$
Gear 2 nd order		$2\Delta t/(3C)$	$-(2C/\Delta t) \cdot u_{ij}(t-\Delta t) - (C/2\Delta t) u_{ij}(t-2\Delta t)$



MULTYCAB

February 2015 Deliverable 2

Document	Deliverable 2
Facilities	-
Revision	Revised
Date	February 2015

Nodal circuit analysis



6 Nodal analysis combining R, L and C elements

As explained, R, L and C elements will be represented as an equivalent circuit of resistive branches and current sources. Whereas the resistors have constant values, the equivalent current sources values depend both on time and the previous history, so their values must be updated every time step.

This structure allows to be processed by standard matrix methods, for example by applying the nodal analysis technique, in which a conductance matrix $[G]$ is formed from the inverse resistance value of each branch in the equivalent circuit. It is a square matrix, whose size is determined by the number of nodes in the analyzed circuit. A column matrix $[I]$ is formed where each element consists of the sum of all current sources at a node.

Before applying the nodal analysis technique, all R, L and C elements must be transformed in their Norton representation.

The five steps to solve electrical circuits through nodal analysis:

Step 1.- No voltage sources allowed. In circuits containing voltage sources, they must be converted to current sources by applying the Thevenin-Norton equivalence.

Step 2.- Draw and label nodal voltages. Number each node, except the ground or reference node at the bottom.

Step 3.- Add all conductances attached to each node. At each node, add up the conductance of all the resistors attached to it ($G = 1/R$).

Step 4.- Subtract the conductances placed between nodes.

Step 5.- At each node add the current sources flowing into the node and subtract those flowing out.

Step 6.- Write the equations matrixes and solve the equation:

$$[I] = [1/R] \cdot [U] = [G] \cdot [U]$$

And find the matrix: $[U] = [G]^{-1} \cdot [I]$

6.1 Conductance matrix inversion

Due to the sparse nature of the conductance matrix $[G]$ (it has many elements which are 0.0), instead of calculating the inverse of the conductance matrix ($[G]^{-1}$), it is better to apply the LU decomposition of the $[G]$ matrix, also known as forward triangularization and back-substitution.

6.2 Nodal circuit analysis. Example.

The aim of this section is to solve the circuit shown in Fig. 6.1, which has 3 nodes. Usually such example should consist of 3 voltages to be determined, however due to the voltage source there are 4 unknowns, that is the 3 nodal voltages and the current flowing through the voltage source.

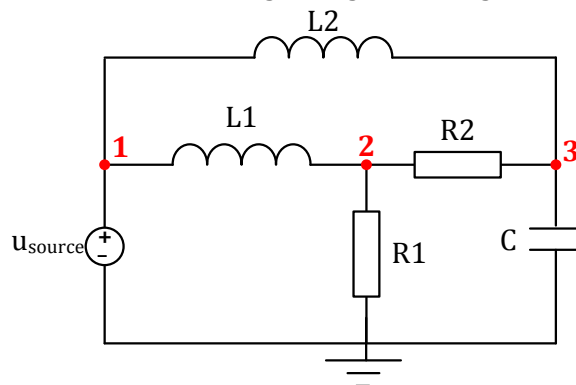


Fig. 6.1. Circuit example 1.

The next step is to convert all elements into their models, as shown in Fig. 6.2.

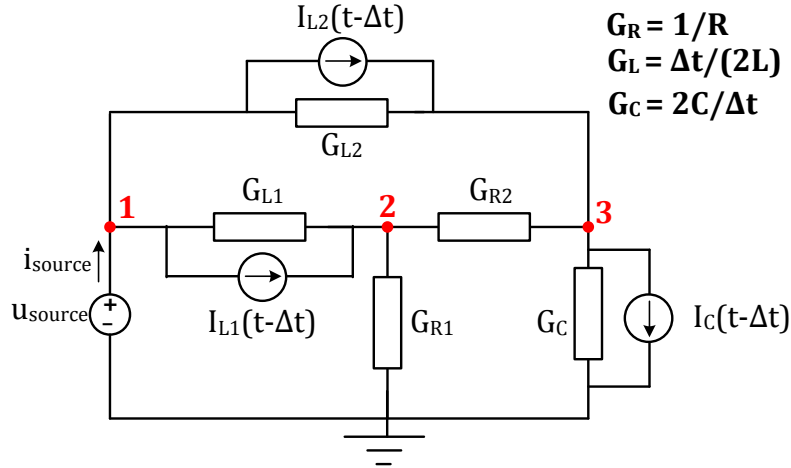


Fig. 6.2. Equivalent circuit.

Now the problem can be formulated in matrix notation as,

$$\begin{bmatrix} G_{L1} + G_{L2} & -G_{L1} & -G_{L2} & 1 \\ -G_{L1} & G_{R1} + G_{R2} + G_{L1} & -G_{R2} & 0 \\ -G_{L2} & -G_{R2} & G_{L2} + G_{R2} + G_C & 0 \\ 1 & 0 & 0 & 0 \end{bmatrix} \begin{bmatrix} u_1(t) \\ u_2(t) \\ u_3(t) \\ i_{source}(t) \end{bmatrix} = \begin{bmatrix} -I_{L1}(t - \Delta t) - I_{L2}(t - \Delta t) \\ I_{L1}(t - \Delta t) \\ I_{L2}(t - \Delta t) - I_C(t - \Delta t) \\ u_{source}(t) \end{bmatrix}$$

Where the history currents are defined as,

$$\begin{aligned}
 I_{L1}(t - \Delta t) &= i_{L1}(t - \Delta t) + G_{L1} \cdot [u_1(t - \Delta t) - u_2(t - \Delta t)] \\
 I_{L2}(t - \Delta t) &= i_{L2}(t - \Delta t) + G_{L2} \cdot [u_1(t - \Delta t) - u_3(t - \Delta t)] \\
 I_C(t - \Delta t) &= -i_C(t - \Delta t) - G_C \cdot u_3(t - \Delta t)
 \end{aligned}$$

Which in simplified form becomes $[G] \cdot [U] = [I]$.

Now matrix $[U]$ must be solved by applying $[U] = [G]^{-1} \cdot [I]$ where the inverse of $[G]$ is calculated through the LU decomposition.

6.3 Longitudinal and transversal impedances of a two-conductors unscreened cable. Single cell model

The full model of a cable includes both the longitudinal and transversal impedances, which are included in this example. The components' values of the single cell equivalent circuit are obtained by applying the recursive GA, and for each parameter the corresponding conductance is calculated ($G_R = 1/R$, $G_L = \Delta t / 2L$, $G_C = 2C / \Delta t$). Let's assume that the circuit in Fig. 6.3 can reproduce the single cell model of a two-conductors unscreened cable, considering both the longitudinal and transversal impedances, and it's connected to a source to do the open circuit test.

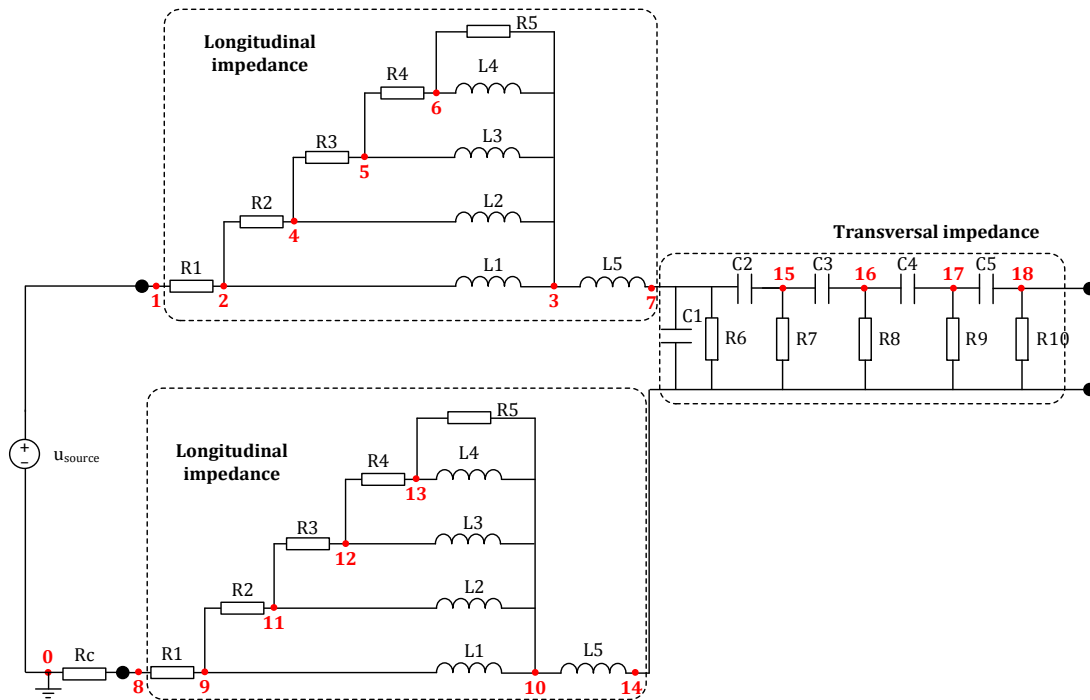


Fig. 6.3. Single cell equivalent circuit considering the longitudinal and transversal.

Where a resistance $R_c \approx 0$ ($1e-12$ Ohm) has been added to the circuit to connect the longitudinal impedance to ground.

Now, the conductance matrix $[G]$ with dimensions 19×19 is as follows,

G1	-G1	0	0	0	0	0	0	0	0	0	0	0	0	0	0	0	0	0	1
-G1	G1+G2+GL1	-GL1	-G2	0	0	0	0	0	0	0	0	0	0	0	0	0	0	0	0
0	-GL1	GL1+GL2+GL3+GL4+GL5+GS	-GL2	-GL3	-GL4-G5	-GL5	0	0	0	0	0	0	0	0	0	0	0	0	0
0	-G2	-GL2	G2+G3+GL2	-G3	0	0	0	0	0	0	0	0	0	0	0	0	0	0	0
0	0	-GL3	-G3	G3+G4+GL3	-G4	0	0	0	0	0	0	0	0	0	0	0	0	0	0
0	0	-GL4-G5	0	-G4	G4+GL4+G5	0	0	0	0	0	0	0	0	0	0	0	0	0	0
0	0	-GL5	0	0	0	GL5+CC1+G6+GC2	0	G1	-G1	0	0	0	0	-GC1-G6	-GC2	0	0	0	0
0	0	0	0	0	0	0	0	-G1	G1+G2+GL1	-GL1	-G2	0	0	0	0	0	0	0	0
0	0	0	0	0	0	0	0	-GL1	GL1+GL2+GL3+GL4+GL5+GS	-GL2	-GL3	-GL4	-GL5	0	0	0	0	0	0
0	0	0	0	0	0	0	0	-G2	-GL2	GL2+G2+G3	-G3	0	0	0	0	0	0	0	0
0	0	0	0	0	0	0	0	-GL3	-GL3	G3+G4+GL3	-G4	0	0	0	0	0	0	0	0
0	0	0	0	0	0	0	0	-GL4-G5	0	-G4	G4+G5+GL4	0	0	0	0	0	0	0	0
0	0	0	0	0	0	-GC1-G6	0	0	-GL5	0	0	0	GL5+GC1+G6+G7+G8+G9+G10	-G7	-G8	-G9	-G10	0	
0	0	0	0	0	0	-GC2	0	0	0	0	0	0	-G7	GC2+G7+GC3	-GC3	-GC4	GC4	0	0
0	0	0	0	0	0	0	0	0	0	0	0	0	-G8	-GC3	GC3+G8+GC4	GC4	0	0	0
0	0	0	0	0	0	0	0	0	0	0	0	0	-G9	0	-GC4	G9+GC4+GC5	-GC5	0	0
0	0	0	0	0	0	0	0	0	0	0	0	0	-G10	0	0	-GC5	GC5+G10	0	0
1	0	0	0	0	0	0	0	0	0	0	0	0	0	0	0	0	0	0	0

In matrix notation it results in,

$$[G] \cdot [U] = [I]$$

where,

$$[U] = \begin{bmatrix} u_1(t) \\ u_2(t) \\ u_3(t) \\ u_4(t) \\ u_5(t) \\ u_6(t) \\ u_7(t) \\ u_8(t) \\ u_9(t) \\ u_{10}(t) \\ u_{11}(t) \\ u_{12}(t) \\ u_{13}(t) \\ u_{14}(t) \\ u_{15}(t) \\ u_{16}(t) \\ u_{17}(t) \\ u_{18}(t) \\ i_{source}(t) \end{bmatrix}$$

$$[I] = \begin{bmatrix} 0 \\ -I_{L1_c1}(t - \Delta t) \\ I_{L1_c1}(t - \Delta t) + I_{L2_c1}(t - \Delta t) + I_{L3_c1}(t - \Delta t) + I_{L4_c1}(t - \Delta t) - I_{L5_c1}(t - \Delta t) \\ -I_{L2_c1}(t - \Delta t) \\ -I_{L3_c1}(t - \Delta t) \\ -I_{L4_c1}(t - \Delta t) \\ I_{L5_c1}(t - \Delta t) - I_{C1}(t - \Delta t) - I_{C2}(t - \Delta t) \\ 0 \\ -I_{L1_c2}(t - \Delta t) \\ I_{L1_c2}(t - \Delta t) + I_{L2_c2}(t - \Delta t) + I_{L3_c2}(t - \Delta t) + I_{L4_c2}(t - \Delta t) - I_{L5_c2}(t - \Delta t) \\ -I_{L2_c2}(t - \Delta t) \\ -I_{L3_c2}(t - \Delta t) \\ -I_{L4_c2}(t - \Delta t) \\ I_{L5_c2}(t - \Delta t) + I_{C1}(t - \Delta t) \\ I_{C2}(t - \Delta t) - I_{C3}(t - \Delta t) \\ I_{C3}(t - \Delta t) - I_{C4}(t - \Delta t) \\ I_{C4}(t - \Delta t) - I_{C5}(t - \Delta t) \\ I_{C5}(t - \Delta t) \\ u_{source} \end{bmatrix}$$

Where sub-indexes $_c1$ and $_c2$ refer to conductors 1 and 2, respectively and $\Delta t = 1e-11$ s

The history currents are defined as,

For inductors:

$$\begin{aligned}
 I_{L1_c1}(t - \Delta t) &= i_{L1_c1}(t - \Delta t) + G_{L1} \cdot [u_2(t - \Delta t) - u_3(t - \Delta t)] \\
 I_{L2_c1}(t - \Delta t) &= i_{L2_c1}(t - \Delta t) + G_{L2} \cdot [u_4(t - \Delta t) - u_3(t - \Delta t)] \\
 I_{L3_c1}(t - \Delta t) &= i_{L3_c1}(t - \Delta t) + G_{L3} \cdot [u_5(t - \Delta t) - u_3(t - \Delta t)] \\
 I_{L4_c1}(t - \Delta t) &= i_{L4_c1}(t - \Delta t) + G_{L4} \cdot [u_6(t - \Delta t) - u_3(t - \Delta t)] \\
 I_{L5_c1}(t - \Delta t) &= i_{L5_c1}(t - \Delta t) + G_{L5} \cdot [u_3(t - \Delta t) - u_7(t - \Delta t)] \\
 I_{L1_c2}(t - \Delta t) &= i_{L1_c2}(t - \Delta t) + G_{L1} \cdot [u_9(t - \Delta t) - u_{10}(t - \Delta t)] \\
 I_{L2_c2}(t - \Delta t) &= i_{L2_c2}(t - \Delta t) + G_{L2} \cdot [u_{11}(t - \Delta t) - u_{10}(t - \Delta t)] \\
 I_{L3_c2}(t - \Delta t) &= i_{L3_c2}(t - \Delta t) + G_{L3} \cdot [u_{12}(t - \Delta t) - u_{10}(t - \Delta t)] \\
 I_{L4_c2}(t - \Delta t) &= i_{L4_c2}(t - \Delta t) + G_{L4} \cdot [u_{13}(t - \Delta t) - u_{10}(t - \Delta t)] \\
 I_{L5_c2}(t - \Delta t) &= i_{L5_c2}(t - \Delta t) + G_{L5} \cdot [u_{10}(t - \Delta t) - u_{14}(t - \Delta t)]
 \end{aligned}$$

For capacitors:

$$\begin{aligned}
 I_{C1}(t - \Delta t) &= -i_{C1}(t - \Delta t) - G_{C1} \cdot [u_7(t - \Delta t) - u_{14}(t - \Delta t)] \\
 I_{C2}(t - \Delta t) &= -i_{C2}(t - \Delta t) - G_{C2} \cdot [u_7(t - \Delta t) - u_{15}(t - \Delta t)] \\
 I_{C3}(t - \Delta t) &= -i_{C3}(t - \Delta t) - G_{C3} \cdot [u_{15}(t - \Delta t) - u_{16}(t - \Delta t)] \\
 I_{C4}(t - \Delta t) &= -i_{C4}(t - \Delta t) - G_{C4} \cdot [u_{16}(t - \Delta t) - u_{17}(t - \Delta t)] \\
 I_{C5}(t - \Delta t) &= -i_{C5}(t - \Delta t) - G_{C5} \cdot [u_{17}(t - \Delta t) - u_{18}(t - \Delta t)]
 \end{aligned}$$



MULTYCAB

February 2015 Deliverable 2

Document	Deliverable 2
Facilities	-
Revision	Revised
Date	February 2015

Conclusions



Document	Deliverable 2
Facilities	-
Revision	Revised
Date	February 2015

7 Conclusions

This deliverable has reviewed different aspects of the MultyCaB project including:

- The cable configurations to be analyzed have been stated.
- A seven steps method to generate and solve the cable model has been established.
- The wide-frequency longitudinal and transversal impedances model of the cable, which include eddy currents effects, inductive and capacitive couplings between conductors and between conductors and screen have been fully described.
- The experimental setup and the experimental tests to be performed to determine the response of the longitudinal and transversal impedances with frequency have been detailed.
- An iterative Genetic Algorithm approach has been described to determine the components of the longitudinal and transversal impedances, that is, R_i , L_i , C_i and G_i with $i = 1 \dots 5$ or 6 , so that the cell model of the cable can reproduce with fidelity the frequency response.
- Although two cable configurations will be studied in detail, the procedure and the tests required to analyze other cable configurations have been analyzed.
- Since the cable model is based on a large number of R-L-C components, to solve the circuit it is required to deal with differential ordinary equations. Therefore, a transient circuit solver method has been described.
- Finally, the nodal circuit analysis method to solve the cable model has been applied.

Document	Deliverable 2
Facilities	-
Revision	Revised
Date	February 2015

8 References

EMTDC. USER'S GUIDE. A Comprehensive Resource for EMTDC EMTDC Transient Analysis for PSCAD Power System Simulation, 244 Cree Crescent, Winnipeg, Manitoba, Canada R3J 3W1

E. Engin, Extraction of Dielectric Constant and Loss Tangent Using New Rapid Plane Solver and Analytical Debye Modeling for Printed Circuit Boards, IEEE Transactions on Microwave Theory and Techniques, vol. 58, no. 1, pp. 211-220, January 2010

Grzybowski, S. ; Dept. of Electr. & Comput. Eng., Mississippi State Univ., Starkville, MS ; Shrestha, P. ; Cao, L, "Electrical Degradation of High Voltage Cable Insulation Energized by Switching Impulses". Annual Report Conference on Electrical Insulation and Dielectric Phenomena, 2008. CEIDP 2008, pp. 25 – 28. Oct. 2008.

U. S. Gudmundsdóttir, "Modelling of long High Voltage AC cables in Transmission Systems", PhD Thesis, Aalborg University, 2010.

H. De Paula, D. Alves de Andrade, M. L. Ribeiro Chaves, J. L. Domingos, and M. A. Arantes de Freitas, Methodology for Cable Modeling and Simulation for High-Frequency Phenomena Studies in PWM Motor Drives, IEEE Trans. Power Electronics, vol. 23, no. 2, March 2008.

B. K. Sen and R. L. Wheeler, "Skin effects models for transmission line structures using generic spice circuit simulators", IEEE 7th topical Meeting on Electrical Performance of Electronic Packaging, pp. 128–131, 1998.

N. Watson, J. Arrilaga, "Power systems electromagnetic transients simulation", IET power & energy series, no. 39, 2003.

N. Watson, and J. Arrillaga, Power Systems Electromagnetic Transients Simulation IET Power and Energy Series 39, The Institution of Engineering and Technology, London, United Kingdom, 2007.

Y. Weens, Modelisation des cables d'énergie soumis aux contraintes generees par les convertisseurs électroniques de puissance, PhD Thesis report, Université des Sciences et Technologies de Lille, 2006.

M. Moreau, Modélisation haute fréquence des convertisseurs d'énergie. Application à l'étude des émissions conduites vers le réseau, PhD Thesis report, Ecole Centrale De Lille, 2009.